Electronic Supplementary Material (ESI) for Chemical Science.
This journal is © The Royal Society of Chemistry 2020

Supporting Information

Cellular Uptake and Targeting of Low Dispersity, Dual Emissive, Segmented Block Copolymer Nanofibers

Steven T. G. Street,[†,‡,⊥,#] *Yunxiang He,*[†,#] *Xu-Hui Jin,*[†,▽] *Lorna Hodgson,*[‖] *Paul Verkade,*[‖]

and Ian Manners[†,‡,*]

[†] School of Chemistry, University of Bristol, Bristol BS8 1TS, United Kingdom

[‡] Department of Chemistry, University of Victoria, Victoria, BC V8W 3V6, Canada

[▽] School of Chemistry and Chemical Engineering, Beijing Institute of Technology, Beijing, China

[‖] School of Biochemistry, University of Bristol, Bristol BS8 1TD, United Kingdom

* Corresponding Author: imanners@uvic.ca

[#] S. T. G. S and Y. H. contributed equally to this work.

Supplementary Results and Discussion

Cytotoxicity of BD and FA Labelled PDHF-*b*-PEG Triblock Nanofibers

The effects of low dispersity dual-emissive BD-PEG-BD triblock nanofibers (L_n = 85 nm, L_w/L_n = 1.19, σ_L = 38 nm) and FA-PEG-FA triblock nanofibers (L_n = 90 nm, L_w/L_n = 1.11, σ_L = 30 nm) were examined on both cancerous and primary cells. BD-PEG-BD and FA-PEG-FA triblock nanofibers were selected as they contain each of the unimer building blocks used to construct the functional PDHF nanofibers, and therefore allow us to draw conclusions regarding the cytotoxicity of each of these functional unimers in isolation from each other. HeLa cervical carcinoma cells were selected as an example of a cancer cell line which overexpresses folate receptors,[1,2] while WI-38 foetal lung fibroblasts were chosen as an example of primary human cells that lack folate receptors.[3] A combination of 72 h alamarBlue™ and calcein AM assays were used to assess reductive metabolism and cell viability respectively. Samples of 85 nm BD-PEG-BD triblock nanofibers and 90 nm FA-PEG-FA triblock nanofibers were incubated with both cell lines at concentrations ranging from 0 to 100 μg/mL. Analysis of the results suggest that no statistically significant effects on reductive metabolism were observed at any concentration examined (up to 100 μg/mL, Table S3-4, Figure S31A and Figure S32A). Effects on cell viability were similar, with no statistically significant effects observed up to 75 μg/mL, although cell viability for WI-38 cells exposed to BD-PEG-BD triblock nanofibers at 100 μg/mL was 80 % of the control, which was deemed statistically significant (Table S5-6, Figure S31B and Figure S32B). Results for both cell lines and nanofibers were broadly similar and indicated that PDHF-*b*-PEG nanofibers are well tolerated by cells. Furthermore, the addition of either FA or BD to the micelle corona led to no significant increase in the cytotoxicity of the nanofibers, despite potentially altering their biological fate. The results described here indicate that modification of the PEG terminus with BD or FA has little effect on cytotoxicity, and are in line with previous studies on the toxicity of PEG, FA, and BODIPY dyes.[4–9] Considering that most biological applications will be using much lower concentrations than those used in this study (for example the accepted dose of nanoparticles for effective *in vivo* drug delivery is ~1 mg/kg),[10] these results suggest that nanofibers with a π-conjugated PDHF core are appropriate for further biological examination.

Investigation of PDHF Innate Fluorescence in the Presence of Cells

The fluorescence profiles for $PDHF_{13}$-*b*-PEG_{227} nanofibers in aqueous solution (Figure S10-13) revealed spectra typical of PDHF-*b*-PEG nanofibers reported previously,[11] with an

excitation λ_{max} of 375 nm and emission λ_{max} at 420 nm and 445 nm. In contrast to previous data recorded in MeOH/THF (1:1), the emission spectra for FA-PEG-FA triblock nanofibers in water also exhibited a longer wavelength band, with a λ_{max} of 490 nm and a shoulder at 530 nm that is associated with excimer formation[12] and/or keto defects[13] (Figure S10). Whilst the inherent fluorescence of the π-conjugated PDHF nanofiber core was easily visualized inside complex mixtures such as cell media (λ_{ex} = 405 nm, λ_{em} = 415-478 nm, Figure S14), complete fluorescence quenching of the PDHF emission was observed in all experiments involving cells (Figure S33). Flow cytometry results with FA-BD-PEG-BD-FA pentablock nanofibers confirmed that no PDHF fluorescence was observed inside HeLa cells (λ_{ex} = 405 nm, λ_{em} = 450 nm), with the fluorescence intensity histograms almost perfectly overlapping with those of the control cells (Figure S18). Confocal Laser Scanning Microscopy (CLSM) investigations using dual-emissive FA-BD-PEG-BD-FA pentablock nanofibers (Figure S33G-J), revealed both intra- and extra-cellular BD fluorescence. Whilst the extracellular fluorescence emission from BD and PDHF was correlated (Figure S33J, purple regions), no intracellular PDHF emission was detected, only emission from BD. Fluorescence quenching of the PDHF nanofiber core upon cellular internalization is consistent with reports of other π-conjugated materials in the presence of biological matter such as proteins,[14] cations,[15] and folic acid.[16] The unique structure of the nanofibers, with exposed termini of the crystalline PDHF core-forming block could help to facilitate these types of interactions inside cells, where reduced steric shielding from the PEG corona allows for efficient fluorescence quenching. The exact cause of fluorescence quenching in this system is currently unclear, though it might possibly be related to nanofiber fragmentation if this occurs. The nanofibers presented herein might ultimately be of use as fluorescence 'turn-off' sensors,[17] however further research is needed to fully understand the observed results.

FRET Interactions between PDHF and BD, and *In vitro* Fluorescence Quenching

Upon conjugation of the BD dye, FRET interactions were observed between BD and the PDHF core (Figure S10-13). The dye must be located within 10 nm of the core-corona interface, presumably to minimize the unfavorable interactions between the hydrophobic dye and water. Whilst FRET interactions between the terminal BD dye and the π-conjugated PDHF core were observed in pentablock nanofibers bearing BD and FA, FA-PEG-FA triblock nanofibers lacking BD were also unobservable inside cells via fluorescence emission. This indicated that FRET interactions between the two fluorophores cannot explain the observed fluorescence quenching.

Materials and Methods

All reactions were carried out in an MBraun MB150B-G glove box under nitrogen atmosphere or using standard Schlenk line techniques. Solvents for self-assembly were purchased at HPLC grade and filtered through a PTFE membrane with pore size of 450 nm. Anhydrous solvents were obtained using a modified Grubbs system of alumina columns manufactured by Anhydrous Engineering.[18] All reagents and solvents were purchased from Sigma-Aldrich, Acros, Fluka, Fisher Chemical and Alfa Aesar, and used as received unless otherwise noted. Cell culture media and additives were purchased from Gibco (Thermo Fischer Scientific). The Dulbecco's Minimal Essential Medium (DMEM) formulation contained high glucose (4.5 g/L), Sodium Pyruvate (0.11 g/L), GlutaMAX™, and Phenol Red (15 mg/L), and was missing HEPES (catalogue number: 10569044). The Minimal Essential Medium (MEM) formulation contained GlutaMAX™, and Phenol Red (10 mg/L), and was missing HEPES (catalogue number: 41090101). Phosphate Buffered Saline (PBS) contained NaCl (9 g/L), KH_2PO_4 (144 mg/L) and Na_2HPO_4-7.H2O (795 mg/L, catalogue number: 10010049). Accutase® was provided as a solution in Dulbecco's PBS containing EDTA (0.5 mM) and Phenol Red (catalogue number: 00-4555-56). TrypLE Express™ was provided with EDTA (458 mg/L) and without Phenol Red (catalogue number: 12604021).

Instrumentation

Ultrasonication

Micelle sonication was carried out using a Hielschur UP100H sonication probe (100W output power).

NMR Spectroscopy

^{1}H and ^{13}C NMR spectra were obtained using Varian 400 MHz and 500 MHz spectrometers with $CDCl_3$ (^{1}H NMR: δ = 7.26 ppm; ^{13}C NMR δ = 77.16 ppm) or DMSO-d_6 (^{1}H NMR: δ = 2.50 ppm; ^{13}C NMR δ = 35.91 ppm) as solvents, and integrations of all peaks were referenced against the residual solvent peak.

Gel permeation chromatography (GPC)

GPC was conducted on a Viscotek VE2001 GPCmax chromatograph equipped with a refractive indices (RI) and a UV detector array. *n*-Bu_4NBr/THF (0.1 w/w %) was used as the eluent, with the flow rate set at 1 mL/min. The columns used were of grade GP5000HHR followed by GP2500HHR (Viscotek) at a constant temperature of 30 °C. The calibration of the

RI detector was carried out using polystyrene standards (Viscotek). Samples were prepared at 2 mg/mL in eluent and filtered through a Ministart SRP 15 filter (polytetrafluorethylene membrane, pore size = 0.45 μm).

Matrix-assisted laser desorption/ionization time of flight mass spectrometry (MALDI-TOF MS)

MALDI-TOF MS measurements were performed using a Bruker Ultraflextreme running in reflector mode. Samples were prepared using a *trans*-2-[3-(4-*tert*-butylphenyl)-2-methyl-2-propenylidene]malononitrile matrix (20 mg/mL in THF) and the polymer sample (2 mg/mL in THF), mixed in a 10:1 (*v*/*v*) ratio. Approximately 1 μL of the mixed solution was deposited onto a stainless-steel sample plate and allowed to dry in air.

Transmission electron microscopy (TEM)

TEM images were obtained on a JEOL 1400 microscope with a SIS MegaViewIII digital camera, which was operated at 120 kV. Samples were prepared by drop casting 4 μL of the micelle solution onto a carbon coated copper grid. Copper grids (400 mesh) were purchased from Agar Scientific and carbon films were prepared on mica sheets by carbon sputtering with an Agar TEM Turbo Carbon Coater. The carbon films were deposited onto the copper grids by floatation on water and the carbon coated grids were allowed to dry in air.

For micelle contour lengths analysis, ca. 200 micelles in several images were traced manually using the Fiji (ImageJ) software package developed at the US National Institute of Health. The number average micelle length (L_n) or width (W_n) and weight average micelle length (L_w) or width (W_w) were calculated using eq. S1 from measurements of the contour lengths/widths (L_i) of individual micelles, where N_i is the number of micelles of length L_i, and n is the number of micelles examined in each sample. The distribution of micelle lengths/widths is characterized by both L_w/L_n (or W_w/W_n) and σ (standard deviation).

$$L_n = \frac{\sum_{i=1}^{n} N_i L_i}{\sum_{i=1}^{n} Ni} \qquad L_w = \frac{\sum_{i=1}^{n} N_i L_i^2}{\sum_{i=1}^{n} NiLi} \qquad \text{(eq.1)}$$

ζ-Potential Measurements

ζ-potential measurements were recorded on a Brookhaven ZetaPALS potential analyzer, following the Smoluchowski approximation at 25 °C. Samples were diluted to 5 μg/mL in 5 mM NaCl buffer, with each cuvette containing 1400 μL of micelle solution. A minimum of

four measurements per sample were taken, each consisting of 30 cycles per run. The average ζ-potential from each sample was taken, with error represented as σ.

Absorbance and Fluorescence Measurements

Absorbance spectra were recorded on a Cary 100 UV-Vis spectrophotometer. Steady-state fluorescence measurements were performed on a PTI QM-40 spectrofluorometer. Emission spectra were obtained following excitation at either 375 nm (corresponding to excitation of PDHF), 405 nm (the wavelength used to excite PDHF in CLSM experiments), or 633 nm (corresponding to excitation of BODIPY$^{630/650\text{-X}}$), and the emission was collected between 390-740 nm, 420-750 nm, or 645-750 nm respectively. Excitation spectra were recorded for the emission maxima at 420 nm, 445 nm, 475 nm, 490 nm, 530 nm, 575 nm and 650 nm, collecting data between 230-405 nm, 230-430 nm, 245-460 nm, 255-470 nm, 275-520 nm, 300-560 nm, and 335-640 nm respectively. A bandwidth of 2 nm was used for the excitation and emission monochromators, with the gain set to 0.99 V at 375 nm (4.35). Data was collected every 0.5 nm, with samples in a low-volume 2 × 10 mm quartz fluorescence cuvette (Hellma Analytics). The volume of sample used was 150 μL. A baseline spectrum for water was subtracted from all emission spectra to obtain corrected spectra, and where appropriate data was normalized using GraphPad Prism 8 (GraphPad Software). All measurements were performed by maintaining the sample temperature at 20 °C.

Confocal Laser Scanning Microscopy (CLSM)

CLSM imaging was performed in the Wolfson Bioimaging Facility at the University of Bristol on a Lecia SP8 AOBS confocal laser scanning microscope attached to a Lecia DM I6000 inverted epifluorescence microscope with 'Adaptive Focus Control' to correct focus drift during time-courses (BBSRC Alert 13 capital grant (BB/L014181/1). All images were taken at 37 °C using a 40× or 63× 1.4 oil-immersion lens. Excitation lasers were operated at 405 nm for PDHF and DAPI, 488 nm for GFP and Alexa Fluor 488 Phalloidin, and either 561 nm or 633 nm for BODIPY$^{630/650\text{-X}}$. Confocal images were obtained using digital detectors with observation windows of 415-478 nm for PDHF and DAPI, 498-551 nm for GFP and Alexa Fluor 488 Phalloidin, and either 571-670 nm or 640-700 nm for BODIPY$^{630/650\text{-X}}$. The images were processed using LAS X (Lecia) and Fiji software (ImageJ).

Correlative Light and Electron Microscopy (CLEM)

CLEM studies were conducted using the procedure described on pS18, and cells were imaged according to the CLSM and TEM sections. High-resolution composite TEM images used in

CLEM were prepared using ICE 2.0 (Microsoft Image Composite Editor 2.0, Microsoft Corporation). CLSM and TEM data was overlaid using the eC-CLEM plugin[19] for Icy (http://icy.bioimageanalysis.org/).[20]

Flow Cytometry

Flow cytometry was conducted at the University of Bristol Flow Cytometry Facility, on a BD LSR II flow cytometer (BD Biosciences), and data was analyzed using FlowJo v10 software (BD Biosciences, Ashland, Oregon, USA). The 405 nm laser was used to excite PDHF, with the emission being measured using a 450/50 nm band pass filter (BP). The 633 nm laser was used to excite BODIPY$^{630/650\text{-}X}$ and emission was monitored using a 660/20 nm BP. A total of three independent repeats were conducted for each sample, with a minimum of 10,000 cells counted for each repeat. The cells were gated for cells, then single cells, then live cells, before being gated for either PDHF positive or BODIPY$^{630/650\text{-}X}$ positive cells.

Synthesis procedures

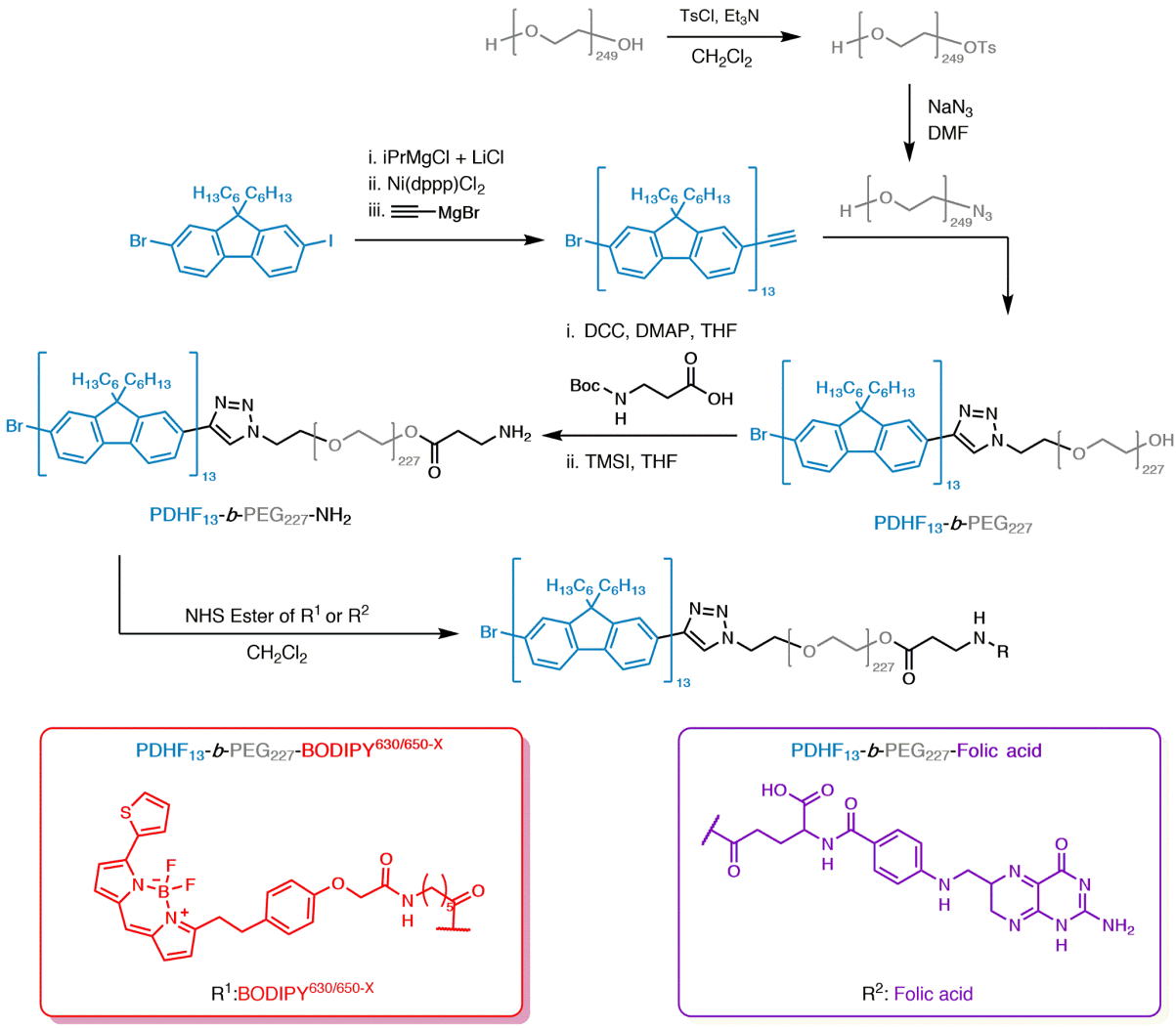

Scheme S1. Synthesis of functionalized PDHF-based diblock copolymers.

Synthesis of alkyne-terminated poly(di-*n*-hexylfluorene) (PDHF$_{13}$-alkyne). The monomer 2-Bromo-7-iodo-9,9-bis-*n*-hexylfluorene and alkyne-terminated PDHF$_{13}$ was synthesized according to the reported procedure.[11] To a solution of 2-Bromo-7-iodo-9,9-bis-*n*-hexylfluorene[21] (1.00 g, 1.85 mmol) in dry THF, *i*-PrMgCl/LiCl (1:1) (1.45 ml, 1.89 mmol, 1.3 M) was added dropwise at -78 °C. The reaction mixture was stirred for 70 min and warmed up to 23 °C, followed by quick transfer to a solution of Ni(dppp)Cl$_2$ (56 mg, 0.103 mmol) in dry THF (100 mL) at 0 °C. After 10 min, the reaction mixture was quenched with an excess of ethynylmagnesium chloride (0.5 M in THF, 3 ml) and stirred for another 60 min. The reaction solution was precipitated in MeOH to afford the PDHF$_{13}$-alkyne as a yellow-green solid. Alkyne-terminated PDHF$_{13}$ was then further purified by Soxhlet extraction with methanol, hexanes, and chloroform (282 mg, 46%). ^{1}H NMR (400 MHz; CD_2Cl_2): δ (ppm) 7.96-7.77 (m,

26H, Ar), 7.75-7.59 (m, 52H, Ar), 2.29-1.94 (m, 52H, alkyl chain), 1.83-0.50 (m, 260H, alkyl chain). MALDI *m/z*: $[M]^+$ found: 4425.76, DP_n: 13. GPC (*n*-Bu_4NBr/THF, PS standard): M_n = 8700 g/mol, $Đ_M$ = 1.22.

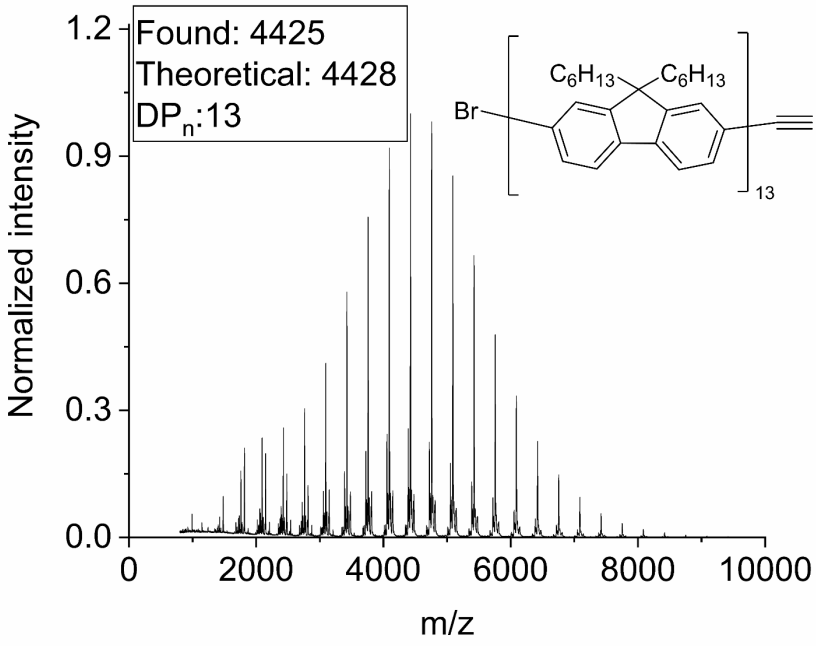

Figure S1. MALDI-TOF MS spectra of alkyne-terminated $PDHF_{13}$.

Synthesis of monosubstituted PEG homopolymer (HO-PEG_{249}-OTs). Under N_2 atmosphere, PEG (HO-PEG_{249}-OH) (5 g, 0.5 mmol) and TEA (210 uL, 1.5 mmol) was dissolved in dry CH_2Cl_2 (100 mL) in a Schlenk flask and cooled to 0 °C. 4-Toluenesulfonyl chloride (TsCl, 40 mg, 0.2 mmol) was dissolved in dry CH_2Cl_2 (50 mL) in another Schlenk flask under N_2. The TsCl solution was transferred dropwise into the HO-PEG_{249}-OH solution at 0 °C. The reaction was stirred for 16 h, followed by precipitation in cold diethyl ether. The product was collected as a white powder which was a mixture of HO-PEG-OH and HO-PEG-OTs (5 g, 99%). MALDI *m/z*: $[M]^+$ found: 11162.12 (HO-PEG_{249}-OTs), 11007.58 (OH-PEG_{249}-OH). MALDI-TOF MS confirmed the presence of monosubstituted HO-PEG_{249}-OTs and absence of di-substituted TsO-PEG-OTs.

Synthesis of monosubstituted PEG homopolymer (HO-PEG_{249}-N_3). HO-PEG_{249}-OTs (HO-PEG_{249}-OH) (5 g, 0.5 mmol, ca. 0.1 mmol of OTs) was dissolved in DMF, followed by addition of NaN_3 (32 mg, 0.5 mmol). The reaction was stirred at 80 °C for 16 h. The reaction was precipitated in cold diethyl ether and dried under vacuum. The product was collected as a white powder which was a mixture of HO-PEG-OH and HO-PEG-N_3 (5 g, 99%). MALDI *m/z*:

$[M]^+$ found: 11077.27 ($HO\text{-}PEG_{249}\text{-}N_3$), 11007.58 ($OH\text{-}PEG_{249}\text{-}OH$). MALDI-TOF MS confirmed the presence of monosubstituted $HO\text{-}PEG_{249}\text{-}N_3$ and absence of di-substituted $TsO\text{-}PEG_{249}\text{-}OTs$ and monosubstituted $HO\text{-}PEG_{249}\text{-}OTs$.

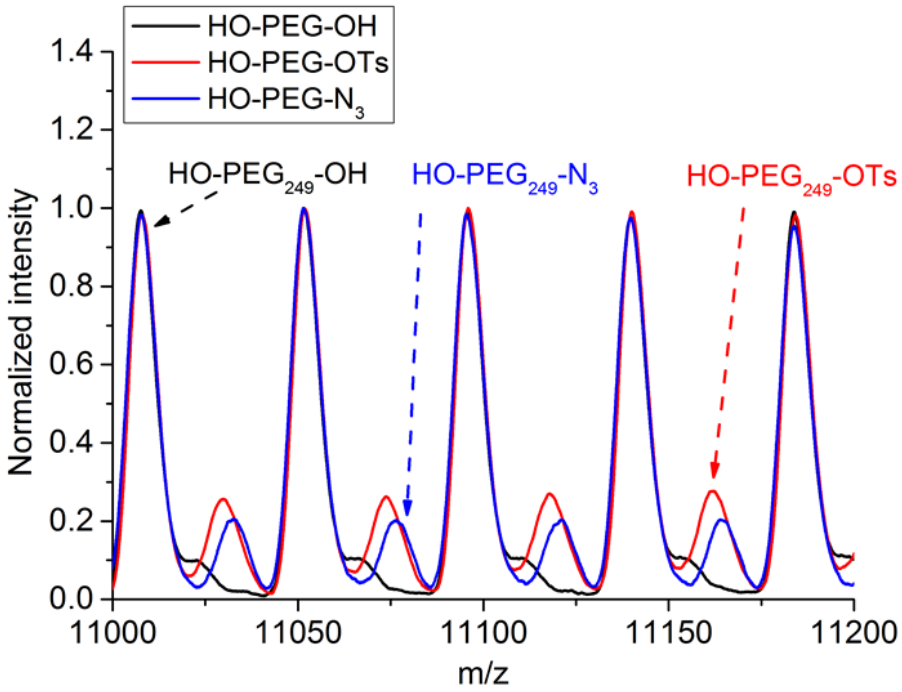

Figure S2. Overlaid MALDI-TOF MS spectra showed the mixture of monosubstituted PEG and unsubstituted PEG. The di-substituted by-product was not observed.

Synthesis of $PDHF_{13}$-*b*-PEG_{227}-OH. To a solution of $PDHF_{13}$-alkyne (20 mg, 5 μmol) and $PEG\text{-}N_3$ (mixed with HO-PEG-OH, 500 mg, 50 μmol) in dry THF (3 mL) in a Schlenk flask, a pre-mixed solution (1 mL, in THF) of CuBr (10 mg, 0.07 mmol) and pentamethyldiethylenetriamine (PMDETA, 15 μL, 0.07 mmol) was added in under a N_2 atmosphere. The reaction mixture was stirred at 40 °C for 48 h. Copper/PMDETA complex was removed by passing the reaction mixture through a basic alumina column. The cured product was precipitated in cold diethyl ether to afford the white solid. The white solid was washed with MeOH to remove excess HO-PEG-OH. The final product was collected by precipitation in cold diethyl ether as a light yellow solid (35 mg, 50%). ^{1}H NMR (400 MHz; CD_2Cl_2): δ (ppm) 7.86-7.84 (m, 26H, Ar), 7.71-7.68 (m, 52H, Ar), 3.64 (s, 910H, $C\underline{H_2}C\underline{H_2}O$ of PEG), 2.14-2.08 (m, 52H, alkyl chain), 1.14-0.78 (m, 260H, alkyl chain). M_n = 14,316 g/mol. GPC (*n*-Bu_4NBr/THF, PS standard): M_n = 29900 g/mol, $Đ_M$ = 1.12.

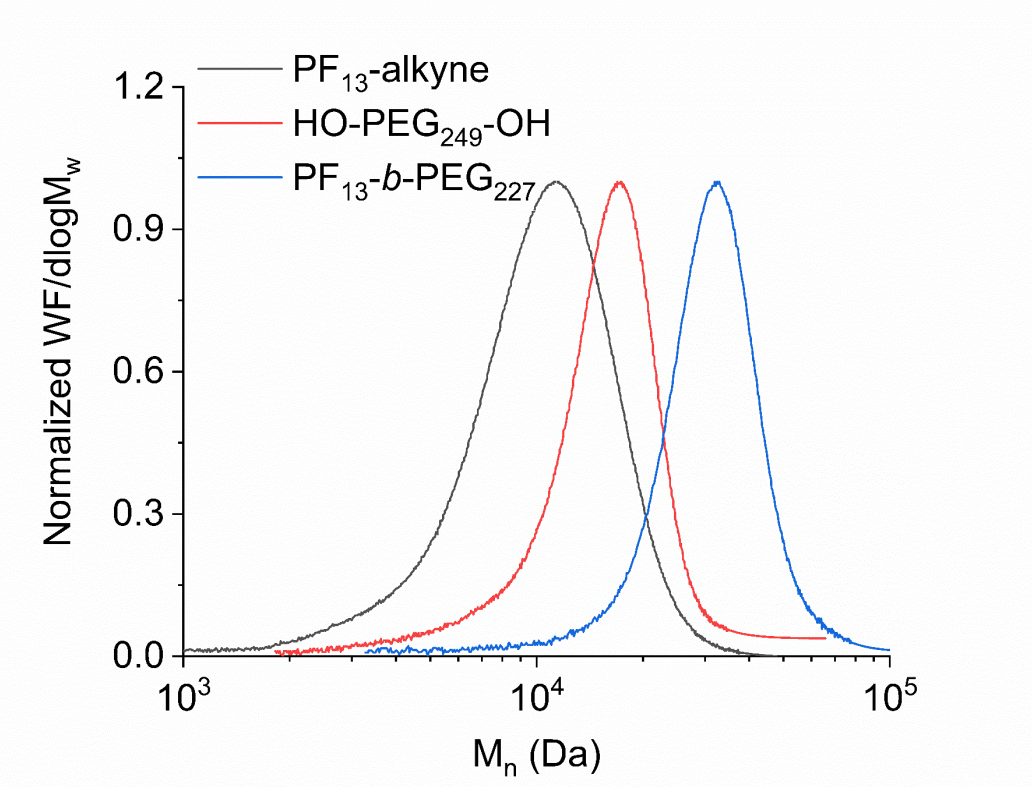

Figure S3. GPC chromatographs (refractive index trace) in 0.1 wt % *n*-Bu_4NBr/THF of PDHF-containing polymers.

Synthesis of $PDHF_{13}$-*b*-PEG_{227}-NHBoc. $PDHF_{13}$-*b*-PEG_{227}-OH (30 mg, 2.1 μmol), Boc-β-alanine (5 mg, 26 μmol), DCC (10 mg, 21 μmol) and DMAP (3 mg, 24 μmol) were dissolved in dry THF (3 mL) in a Schlenk flask. The reaction mixture was stirred at 23 °C for 48 h. The reaction solution was precipitated in hexane (3 × 30 mL) and dried under vacuum for 16 h to afford the product as a light yellow solid (30 mg, 99%). ^{1}H NMR (400 MHz; CD_2Cl_2): δ (ppm) 7.86-7.84 (m, 26H, Ar), 7.71-7.68 (m, 52H, Ar), 3.64 (s, 910H, $C\underline{H_2}C\underline{H_2}O$ of PEG), 2.14-2.08 (m, 52H, alkyl chain), 1.44 (s, 9H, Boc), 1.14-0.78 (m, 260H, alkyl chain). After the confirmation of presence of Boc, the product was used in the next step immediately.

Synthesis of $PDHF_{13}$-*b*-PEG_{227}-NH_2. To a solution of $PDHF_{13}$-*b*-PEG_{227}-NHBoc (30 mg, 2.1 μmol) in dry THF (3 mL) in a Schlenk flask, iodotrimethylsilane (TMSI,) was added under a N_2 atmosphere. The reaction mixture was stirred at 23 °C for 2 h. The reaction solution was precipitated in hexane (3 × 30 mL) and then dried under vacuum for 16 h to afford a yellow solid (30 mg, 99%). ^{1}H NMR (400 MHz; CD_2Cl_2): δ (ppm) 7.86-7.84 (m, 26H, Ar), 7.71-7.68 (m, 52H, Ar), 3.64 (s, 910H, $C\underline{H_2}C\underline{H_2}O$ of PEG), 2.14-2.08 (m, 52H, alkyl chain), 1.14-0.78 (m, 260H, alkyl chain). The product was used in the next step immediately after the absence of the Boc group was confirmed by ^{1}H NMR.

Synthesis of functional $PDHF_{13}$-*b*-PEG_{227}. $PDHF_{13}$-*b*-PEG_{227}-$BODIPY^{630/650\text{-}X}$ is used as an example for the typical procedure of preparing functional PDHF-*b*-PEG diblock polymers. $PDHF_{13}$-*b*-PEG_{227}-NH_2 (10 mg, 0.7 μmol) and $BODIPY^{630/650\text{-}X}$ NHS ester (0.5 mg, 0.75 μmol) were dissolved in dry CH_2Cl_2 (1 mL). The mixture was stirred at 23 °C for 16 h. The reaction solution contents were precipitated in hexane until no fluorescence could be detected under UV light in the supernatant. The polymer was dried in vacuo to afford product as a blue solid (10 mg, 96%). ^{1}H NMR (400 MHz; CD_2Cl_2): δ (ppm) 6.79 (m, 1H, Ar of dye). 6.62 (m, 1H, Ar of dye), 6.39 (m, 1H, Ar of dye), 6.18 (m, 1H, Ar of dye), 7.86-7.84 (m, 26H, Ar), 7.71-7.68 (m, 52H, Ar), 3.64 (s, 910H, $C\underline{H_2}C\underline{H_2}O$ of PEG), 2.14-2.08 (m, 52H, alkyl chain), 1.70-0.78 (m, 260H, alkyl chain). See Figure S4d.

For $PDHF_{13}$-*b*-PEG_{227}-Folic acid (FA): 10 mg, 77%. ^{1}H NMR (400 MHz; DMSO-d_6): δ (ppm) 8.64 (s, 1H, NH), 7.64 (m, 1H, Ar of FA), 6.63 (m, 1H, Ar of FA), 3.53 (s, 910H, $C\underline{H_2}C\underline{H_2}O$ of PEG). See Figure S4c.

(a)

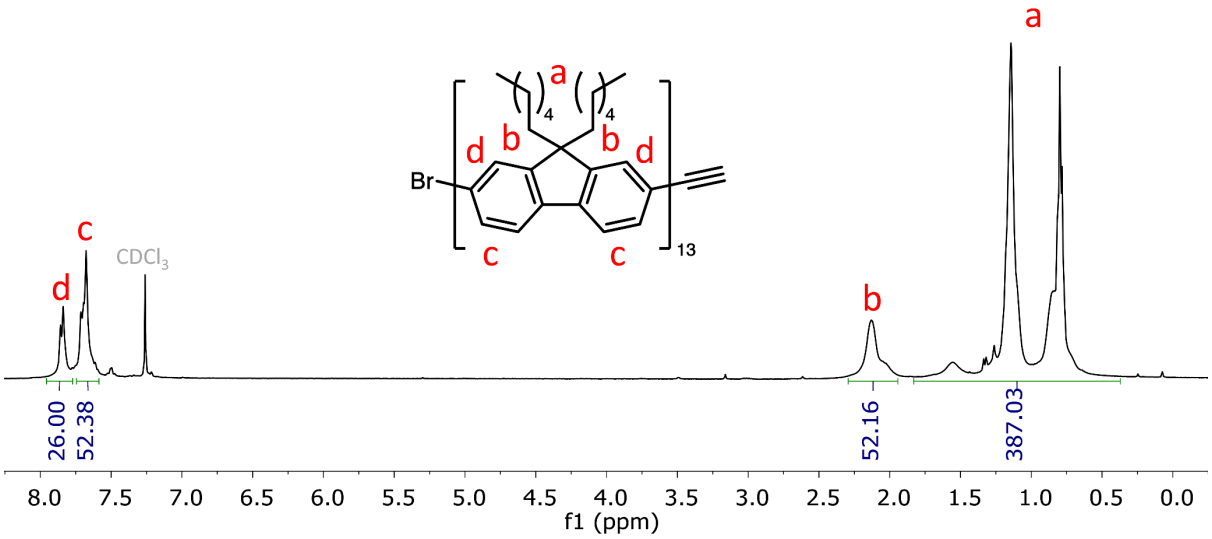
a
b
c
d
CDCl3
Br
13
26.00
52.38
52.16
387.03
f1 (ppm)

(b)

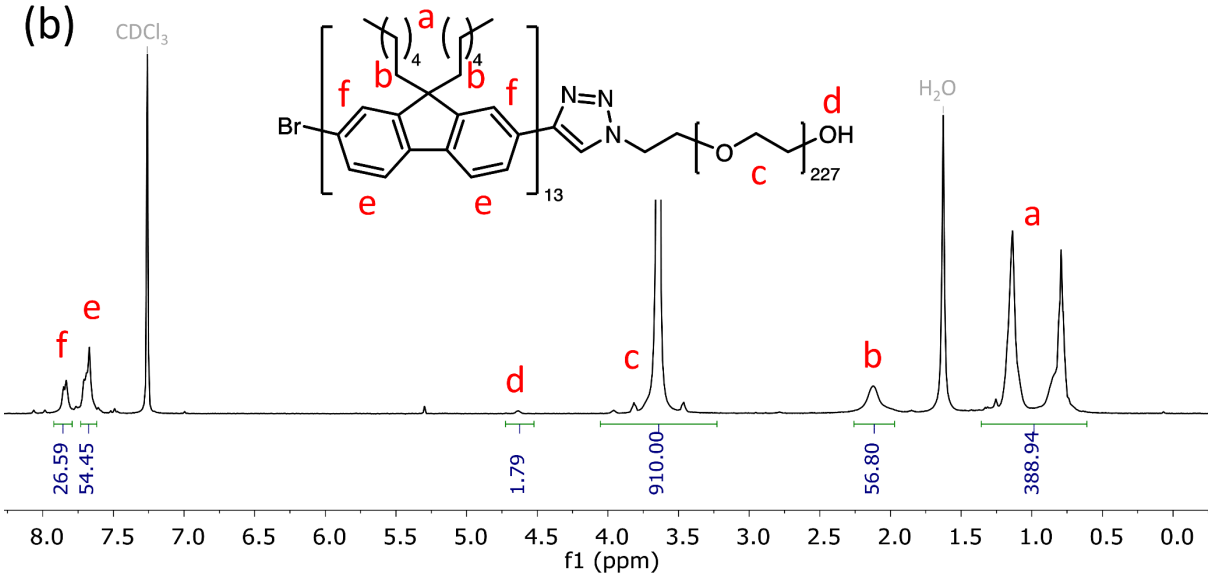
CDCl3
H2O
a
b
c
d
e
f
Br
N=N
OH
227
13
26.59
54.45
1.79
910.00
56.80
388.94
f1 (ppm)

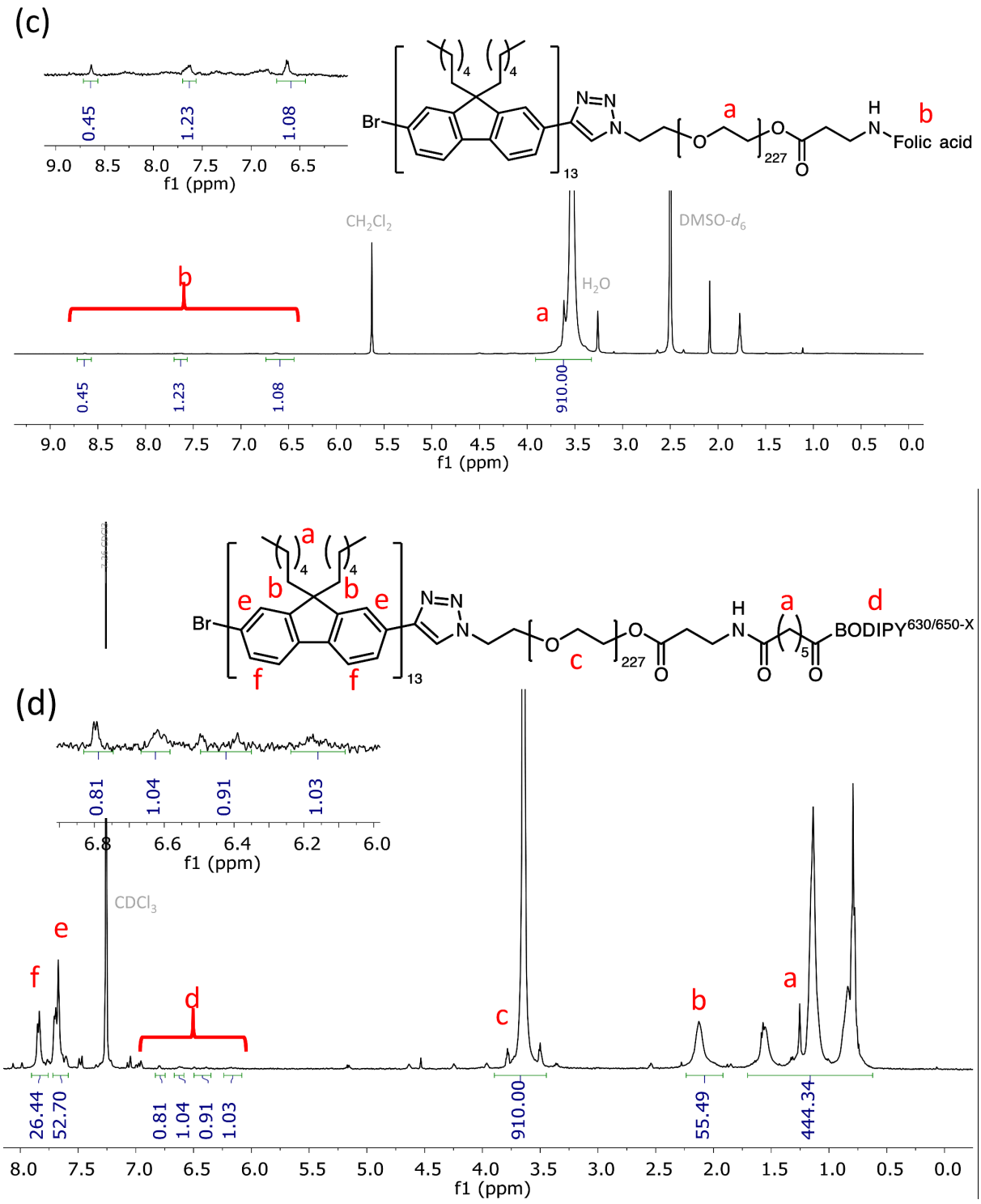

Figure S4. ^{1}H NMR spectra (in $CDCl_3$) of (a) $PDHF_{13}$, (b) $PDHF_{13}$-*b*-PEG_{227}, (c) $PDHF_{13}$-*b*-PEG_{227}-Folic acid (in DMSO-d_6, PDHF signal not present due to self-assembly), and (d) $PDHF_{13}$-*b*-PEG_{227}-$BODIPY^{630/650\text{-}X}$.

Self-assembly procedures

Self-nucleation of $PDHF_{13}$-*b*-PEG_{227}. $PDHF_{13}$-*b*-PEG_{227} (100 μL, 10 mg/mL in THF) was diluted in THF (900 μL). MeOH (1 mL) was added slowly to the THF solution over 10 min at 23 °C. The resulting solution with a concentration of 0.5 mg/mL was manually shaken for 10 s and aged at 23 °C for another 24 h. The formed polydisperse fiber-like micelles were characterized by TEM.

Preparation of $PDHF_{13}$-*b*-PEG_{227} seed micelles. $PDHF_{13}$-*b*-PEG_{227} polydisperse micelles (in MeOH/THF, 1:1) was sonicated for 3 h in a H_2O sonication bath cooled with ice. The resulting micelle solution was characterized by TEM (L_n = 21 nm, L_w/L_n = 1.07, σ = 8 nm).

Preparation of dual emissive, FA functionalized $PDHF_{13}$-*b*-PEG_{227} micelles (FA-BD-PEG-BD-FA Pentablock Nanofiber). $PDHF_{13}$-*b*-PEG_{227} seed micelle solution (400 μL, 0.5 mg/mL, in MeOH/THF, *v*:*v* = 1:1) was diluted in MeOH (600 μL) to which was added THF (720 μL). $PDHF_{13}$-*b*-PEG_{227}-$BODIPY^{630/650\text{-}X}$ unimer (40 μL, 10 mg/mL in THF, m_{unimer}:m_{seed} = 2) was added to the diluted seed solution. The resulting solution in MeOH/THF (8:10) was then manually shaken for 10 s, and aged for 24 h at 23 °C (L_n = 56 nm, L_w/L_n = 1.09, σ = 18 nm). DMSO (200 μL) was then added to the prepared micelle solution, followed by the addition of $PDHF_{13}$-*b*-PEG_{227}-Folic Acid unimer (40 uL, 10mg/mL in DMSO/THF, 1:9 m_{unimer}:m_{seed} = 2), manually shaken for 10 s, and aged for 24 h at 23 °C (L_n = 117 nm, L_w/L_n = 1.05, σ = 25 nm). The prepared micelle solution was then diluted with H_2O (2 mL), followed by dialysis against H_2O (resistance 18.2 MΩ·cm at 25 °C) for 2 days with multiple dialysate changes. The solution was then concentrated to 1 mL under a stream of N_2 gas to afford dual fluorescent folic acid functionalized micelles in H_2O with a concentration at 1 mg/mL. The prepared micelles were characterized by TEM (L_n = 95 nm, L_w/L_n = 1.17, σ_L = 39 nm, W_n = 13 nm, W_w/W_n = 1.02, σ_W = 2 nm), fluorescence spectroscopy (Figure S10), CLSM (Figure S14), and ζ-potential (*app.* ζ-potential = -5.5 ± 2.1 mV).

Preparation of dual emissive functional $PDHF_{13}$-*b*-PEG_{227} micelles (BD-PEG-BD Triblock Nanofibers). $PDHF_{13}$-*b*-PEG_{227} seed micelle solution (400 μL, 0.5 mg/mL, in MeOH/THF, *v*:*v* = 1:1) was diluted in MeOH (600 μL) to which was added THF (720 μL). $PDHF_{13}$-*b*-PEG_{227}-$BODIPY^{630/650\text{-}X}$ unimer (80 μL, 10 mg/mL in THF, m_{unimer}:m_{seed} = 4) was then added to the diluted seed solution. The resulting solution in MeOH/THF (8:10) was then manually shaken for 10 s and aged for 1 d at 23 °C before TEM characterization (L_n = 113 nm, L_w/L_n = 1.10, σ = 36 nm). The prepared micelle solution was then diluted with H_2O (2 mL),

followed by dialysis against H_2O (resistance 18.2 MΩ·cm at 25 °C) for 2 days with multiple dialysate changes. The solution was then concentrated to 1 mL under a stream of N_2 gas to afford dual fluorescent micelles in H_2O with a concentration at ca. 1 mg/mL. The prepared micelles were characterized by TEM (L_n = 85 nm, L_w/L_n = 1.19, σ_L = 38 nm, W_n = 11 nm, W_w/W_n = 1.02, σ_W = 2 nm), fluorescence spectroscopy (Figure S10), CLSM (Figure S14), and ζ-potential (*app.* ζ-potential = -4.2 ± 2.0 mV).

Preparation of FA functionalized $PDHF_{13}$-*b*-PEG_{227} micelles (FA-PEG-FA Triblock Nanofibers). $PDHF_{13}$-*b*-PEG_{227} seed micelle solution (400 μL, 0.5 mg/mL, in MeOH/THF, *v:v* = 1:1) was diluted in MeOH (600 μL) to which was added THF (720 μL). $PDHF_{13}$-*b*-PEG_{227} unimer (40 μL, 10 mg/mL in THF, $m_{unimer}:m_{seed}$ = 2) was added to the diluted seed solution. The resulting solution in MeOH/THF (8:10) was then manually shaken for 10 s and aged for 24 h at 23 °C (L_n = 42 nm, L_w/L_n = 1.07, σ = 12 nm). DMSO (200 μL) was then added to the prepared micelle solution, followed by the addition of $PDHF_{13}$-b-PEG_{227}-Folic Acid unimer (40 μL, 10mg/mL in DMSO/THF, 1:9 $m_{unimer}:m_{seed}$ = 2), manually shaken for 10 s, and aged for 24 h at 23 °C (L_n = 105 nm, L_w/L_n = 1.05, σ = 24 nm). The prepared micelle solution was then diluted with H_2O (2 mL), followed by dialysis against H_2O (resistance 18.2 MΩ·cm at 25 °C) for 2 days with multiple dialysate changes. The solution was then concentrated to 1 mL under a stream of N_2 gas to afford folic acid functionalized micelles in H_2O with a concentration at 1 mg/mL. The prepared micelles were characterized by TEM (L_n = 90 nm, L_w/L_n = 1.11, σ_L = 30 nm, W_n = 12 nm, W_w/W_n = 1.02, σ_W = 2 nm), fluorescence spectroscopy (Figure S10), CLSM (Figure S14), and ζ-potential (app. ζ-potential = -12.4 ± 3.4 mV).

Cell culture protocols

HeLa (Human cervical carcinoma cells) were grown in DMEM media with high glucose (4.5 g/L), and WI-38 (Caucasian fibroblast-like foetal lung cells) were grown in MEM media in a humidified 5% CO_2 incubator at 37°C. All growth media were supplemented with antibiotic-antimycotic agents (to prevent bacterial and fungal contamination) and 10% fetal bovine serum (FBS). Confluent cultures (80% or less) were detached from the surface using trypsin (TrypLE Express™) and plated at 5×10^3 cells/well in 96-well plates for cytotoxicity studies, 2×10^4 cells/well in for CLSM studies, and 5×10^4 cells/well in 24-well plates for flow cytometry.

Cellular uptake experiments

CLSM Studies

For CLSM studies, cells were seeded onto Sarstedt X-Well Coverglass (8 Wells, Base thickness 170μm, Growth Surface 0.8cm, Sarstedt) at a density of 2×10^4 cells per well and incubated overnight before use. Cells were then incubated with 10-100 μg/mL of either BD-PEG-BD triblock nanofibers (L_n = 85 nm, L_w/L_n = 1.19, σ = 38 nm), FA-PEG-FA triblock nanofibers (L_n = 90 nm, L_w/L_n = 1.11, σ = 30 nm), or FA-BD-PEG-BD-FA pentablock nanofibers (L_n = 95 nm, L_w/L_n = 1.17, σ = 39 nm) in medium with reduced FBS (5%) for periods of 0.5-1 h as indicated in the figure legends. At the end of the incubation period, cells were either imaged live, or after fixation using the procedures described below:

For live-cell imaging: at the end of the incubation period the supernatant was removed via aspiration, and the cells were washed with Phosphate-buffered saline (PBS, 200 μL) three times to remove any residual extracellular nanofibers. To the cells, 200 μL of live-cell imaging solution (Molecular Probes, Life Technologies) was added, before imaging by CLSM.

For fixed-cell imaging: at the end of the incubation period the supernatant was removed via aspiration, and the cells were washed with PBS to remove any residual extracellular nanofibers and fixed in 4% paraformaldehyde (PFA) in PBS for 10 minutes. Following a further three washes with PBS, cell membranes were permeabilised with 0.2% saponin in PBS (200 μL) for 10 minutes, before non-specific binding was blocked with 0.1% saponin plus 3% Bovine serum albumin (BSA) in PBS for 30 minutes. Cells were then incubated with DAPI (30 μL of a 1 μg/μL stock, to stain the nuclei) for 5 minutes, and then Alexa Fluor 488 Phalloidin (5 μL of a 6.6 μM stock, to stain F-actin) in PBS (100 μL) for 1 h. The cells were subsequently washed with PBS (200 μL) three times to remove any unbound stain before PBS (200 μL) was added and the sample was imaged by CLSM.

Flow Cytometry Studies

For flow cytometry experiments, cells were seeded at 5×10^4 cells/well in 24-well plates and incubated overnight before use. Cells were then incubated with 10 μg/mL (400 μL) of BD-PEG-BD triblock nanofibers (L_n = 85 nm, L_w/L_n = 1.19, σ = 38 nm) or FA-BD-PEG-BD-FA pentablock nanofibers (L_n = 95 nm, L_w/L_n = 1.17, σ = 39 nm) in medium with FBS (10%) for 45 mins. At the end of the incubation period, cells were washed with PBS, and then Accutase® (with additional HEPES (25 mM) and FBS (2 %)) was added (300 μL), and the

samples aged for 20 minutes at 37 °C. Propidium iodide (PI, 1 μL of 400× solution) was then added to each sample to detect live cells, and the cells were taken for counting on the flow cytometer.

Correlative Light and Electron Microscopy (CLEM)

HeLa cells expressing GRASP65-GFP (with green fluorescent Golgi apparatus for reference)[22] or HeLa cells were plated as for CLSM in imaging dishes containing gridded glass coverslips (MatTek). The cells were cooled to 4 °C using an ice bath, and either FA-BD-PEG-BD-FA pentablock nanofibers (for GRASP65-GFP HeLa, 50 μg/mL, L_n = 95 nm, L_w/L_n = 1.17, σ = 39 nm) or FA-PEG-FA triblock nanofibers (for HeLa, L_n = 90 nm, L_w/L_n = 1.11, σ = 30 nm) in DMEM (200 μL) were added. After 10 minutes incubation, the micelle solution was removed, and the cells were briefly washed with phosphate-buffered saline (PBS, 200 μL) before fixing in 4% EM grade paraformaldehyde (TAAB) in PBS to halt the cell cycle prior to imaging for brightfield and high magnification fluorescence signals. Cells were subsequently located using the grid number of the gridded glass coverslip as described by Olmos et. al.[23] Secondary fixation was performed in 1.5 % glutaraldehyde / 2% paraformaldehyde in 0.1 M PB for 30–60 mins. After fixation, the cells were briefly rinsed in distilled water and post-fixed in 1 % osmium tetroxide for 30 mins, before rinsing in water. Cells were incubated in 3 % Uranyl acetate in water for 20 mins and subsequently dehydrated through an ascending series of ethanol to 100% prior to infiltration with Epoxy resin and polymerisation overnight at 60°C. The coverslips were removed from the resin blocks using pliers after repeated submersion in liquid N_2 and boiling H_2O and washed several times in PBS. The cells of interest were identified by correlating the grid and cell pattern on the surface of the block with previously acquired confocal images. The resin around the area of interest was cut from the block, and further trimmed by hand using a single edged razor blade to form a small trapezoid block face for serial ultrathin sectioning. Using a diamond knife, serial ultrathin sections of 70 nm thicknesses were cut through the entire extent of the cells of interest and collected on 1.5% formvar-coated single slot grids. The sections were counterstained with Uranyl acetate and lead citrate to further enhance contrast prior to imaging in an electron microscope (See TEM section). Movies (and compressed z-stack images) were created from 2D tiff stacks using Fiji software (ImageJ). Nanofiber entry angle analysis was conducted using the 'measure angle' feature of Fiji software (ImageJ), estimating the cell membrane contour and the nanofiber as straight lines. Examples of measurements are given in Figure S25.

Cell Viability Assays

The influence of BD-PEG-BD triblock nanofibers (L_n = 85 nm, L_w/L_n = 1.19, σ = 38 nm) and FA-PEG-FA triblock nanofibers (L_n = 90 nm, L_w/L_n = 1.11, σ = 30 nm) on WI-38 and HeLa cells was evaluated after 72 h of exposure, and analyzed with a dual calcein / alamarBlue™ assay (Table S3-6 and Figure S31-32). Cell survival was quantified by measuring calcein AM fluorescence. The fluorescence, retained within live cells only, results from activity of esterases on the (nonfluorescent) calcein AM (Molecular Probes). Changes in cell metabolism were assessed using alamarBlue™ (AB, Life Technologies), a cytosolic substrate for reductive metabolism (resazurin to resorufin) whose fluorescence spectrum changes on reduction by cytosolic enzymes. WI-38 and HeLa cells were incubated with 0-100 µg/mL of respective $PDHF_{13}$-*b*-PEG_{227} micelle, for 72 h. Each experiment was repeated at least in triplicate in medium with reduced FBS (5%), and each data point was conducted in sextuplicate. Staurosporine (1 µM/mL, Enzo Life Sciences) was used as a positive control. After 72 h, the plates were washed with PBS, and AB (5 % solution) and calcein (3 µM) were added in medium without FBS. After 1 h incubation, the fluorescence of both dyes was read using a plate reader (BMG Labtech CLARIOstar) (AB λ_{ex} = 545 nm, λ_{em} = 590 nm, calcein λ_{ex} = 494 nm, λ_{em} = 517 nm). Results were expressed as percentages of the control and plotted against analyte concentration (in µg/mL). To assess the statistical significance of these results, multiple comparison one-way ANOVA analyses were conducted in GraphPad Prism 7, comparing fluorescence intensity from the cells incubated with $PDHF_{13}$-*b*-PEG_{227} nanofibers to that of the control population.

Supplementary Figures

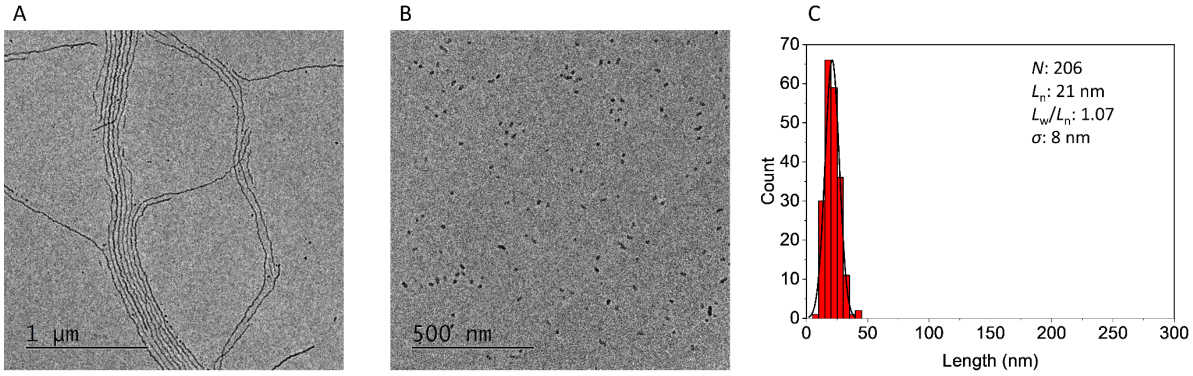

Figure S5. Preparation of $PDHF_{13}$-*b*-PEG_{227} seed micelles. (A) Polydisperse fiber-like micelles of $PDHF_{13}$-*b*-PEG_{227} by direct dissolution in MeOH/THF (1:1) at 0.5 mg/mL at 23 °C. (B) Seed micelles prepared by sonication at 0 °C in a ultrasonic bath for 3h (L_n: 21 nm, L_w/L_n: 1.07, σ = 8 nm). (C) Contour length histogram of seed micelles.

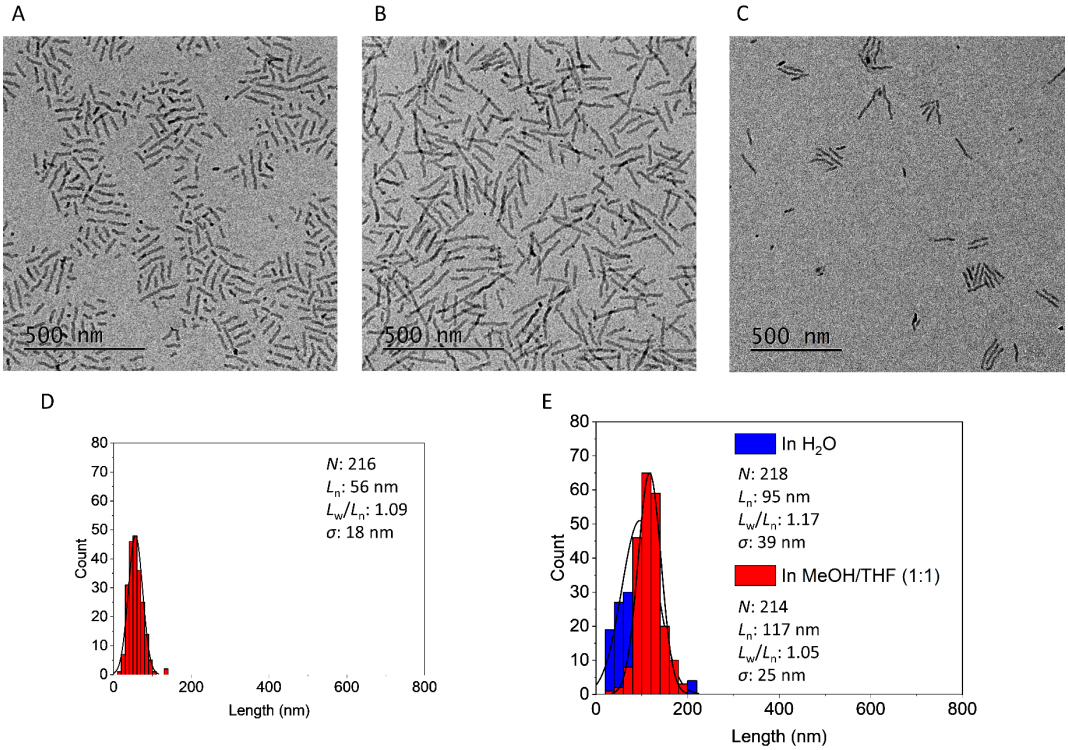

Figure S6. Preparation of FA-BD-PEG-BD-FA pentablock nanofibers. TEM images of (A) BD modified $PDHF_{13}$-*b*-PEG_{227} central segment micelles. TEM images of FA-BD-PEG-BD-FA pentablock nanofibers in (B) MeOH/THF (1:1) and (C) H_2O at 0.5 mg/mL. (D) Contour length histogram of central segment micelles. (E) Comparison between contour length histogram of FA-BD-PEG-BD-FA pentablock nanofibers in MeOH/THF (1:1) and H_2O.

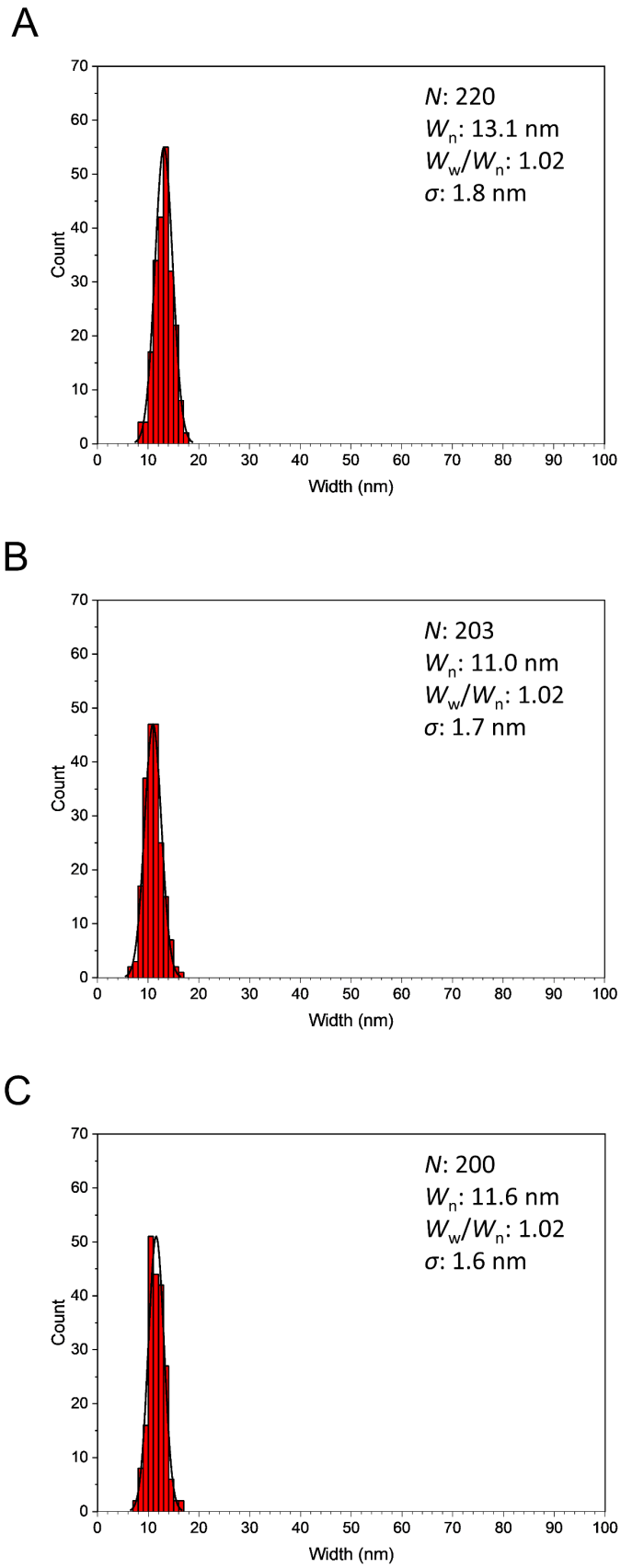

Figure S7. Width measurements of (A) FA-BD-PEG-BD-FA pentablock nanofibers, (B) BD-PEG-BD triblock nanofibers and (C) FA-PEG-FA triblock nanofibers in water.

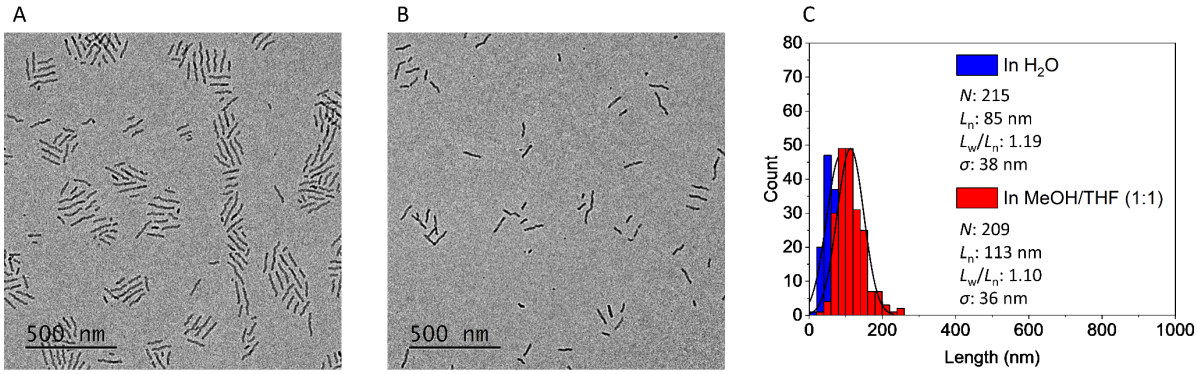

Figure S8. TEM images of BD-PEG-BD triblock nanofibers in (A) MeOH/THF (1:1) and (B) H_2O at 0.5 mg/mL. (C) Comparison between contour length histogram of BD-PEG-BD triblock nanofibers in MeOH/THF 1:1 and H_2O.

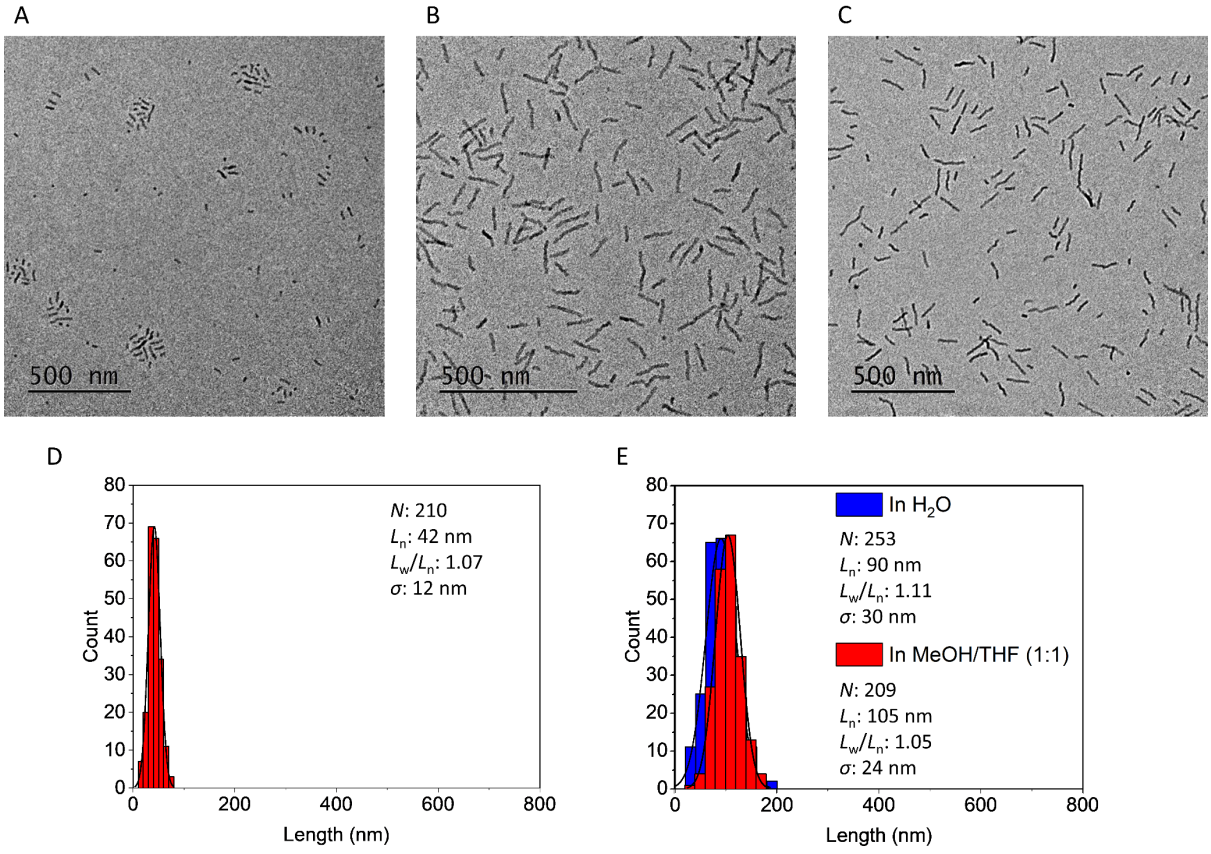

Figure S9. Preparation of FA-PEG-FA triblock nanofibers. TEM images of (A) $PDHF_{13}$-*b*-PEG_{227} central segment micelles. (B-D) TEM images of FA-PEG-FA triblock nanofibers in (B) MeOH/THF (1:1) and (C) H_2O at 0.5 mg/mL. (D) Contour length histogram of central segment micelles. (E) Comparison between contour length histogram of FA-PEG-FA triblock nanofibers in MeOH/THF 1:1 and H_2O.

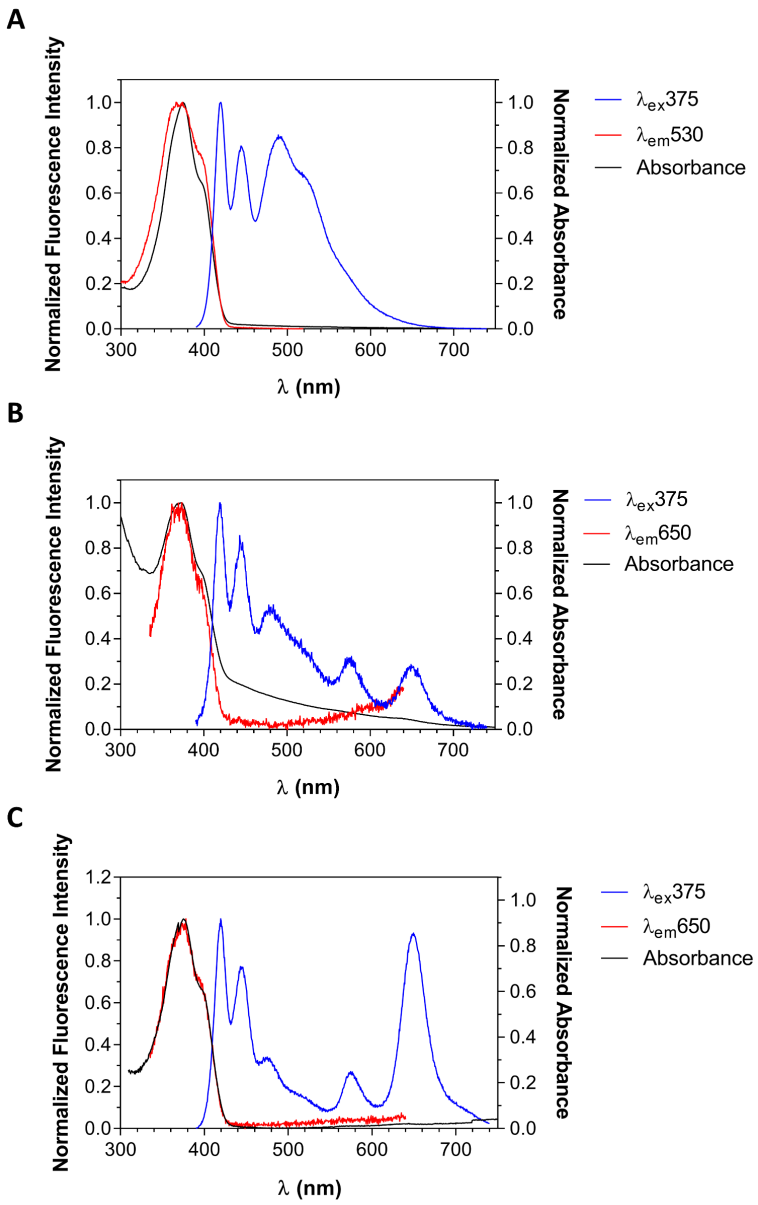

Figure S10. Fluorescence and absorbance spectra of $PDHF_{13}$-*b*-PEG_{227} nanofibers in H_2O. (A) FA-PEG-FA triblock nanofibers (50 µg/mL). (B) BD-PEG-BD triblock nanofibers (500 µg/mL). (C) FA-BD-PEG-BD-FA pentablock nanofibers (50 µg/mL). Note the FRET interaction between the BD dye and the PDHF core (λ_{em} = 650 nm, λ_{ex} = 375 nm) in B and C, which is coupled with a quenching/blue shift of the longer wavelength band present at 490 nm in A, and the appearance of a new emission at 575 nm. These results imply that the terminal BD dye must be in close proximity to the core (<10 nm), presumably at the core-corona interface, with the corona looped back upon itself. $\lambda_{ex}375$ corresponds to the emission profile following excitation at 375 nm, whilst $\lambda_{em}530$ and $\lambda_{em}650$ correspond to the excitation profiles following the emission at either 530 or 650 nm, respectively.

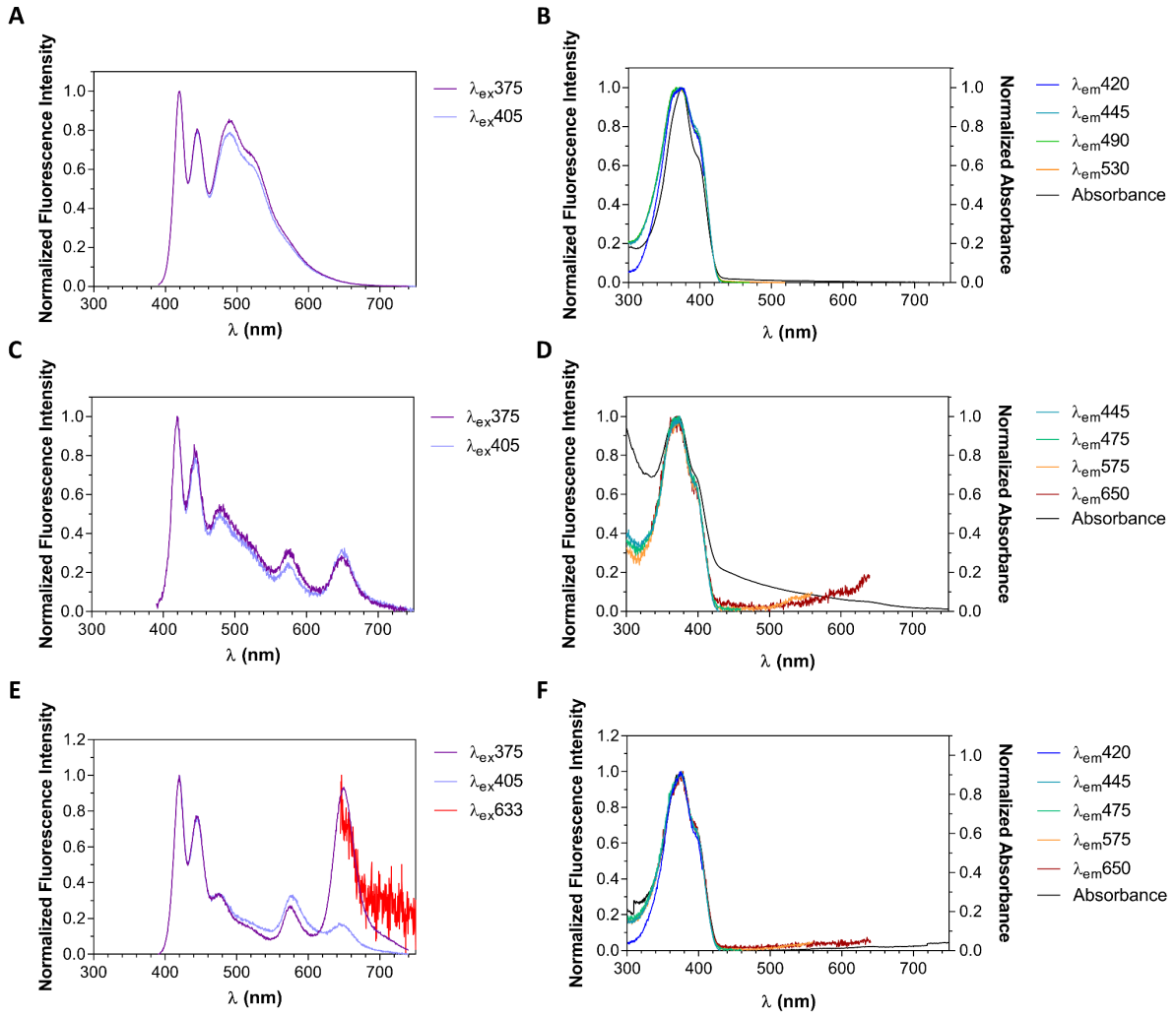

Figure S11. Fluorescence and absorbance spectra of $PDHF_{13}$-*b*-PEG_{227} nanofibers in H_2O at (A, C, E) varied excitation and (B, D, F) emission wavelengths. (A-B) FA-PEG-FA triblock nanofibers (50 µg/mL), (C-D) BD-PEG-BD triblock nanofibers (500 µg/mL), (E-F) FA-BD-PEG-BD-FA pentablock nanofibers (50 µg/mL). Excitation of the PDHF core (λ_{max} = 375 nm) leads to emission at 420 nm, 445 nm, 490 nm and 530 nm (PDHF) and 475 nm, 575 nm, and 650 nm (PDHF/BD). The legend for excitation and emission profiles follows the convention used in Figure S10.

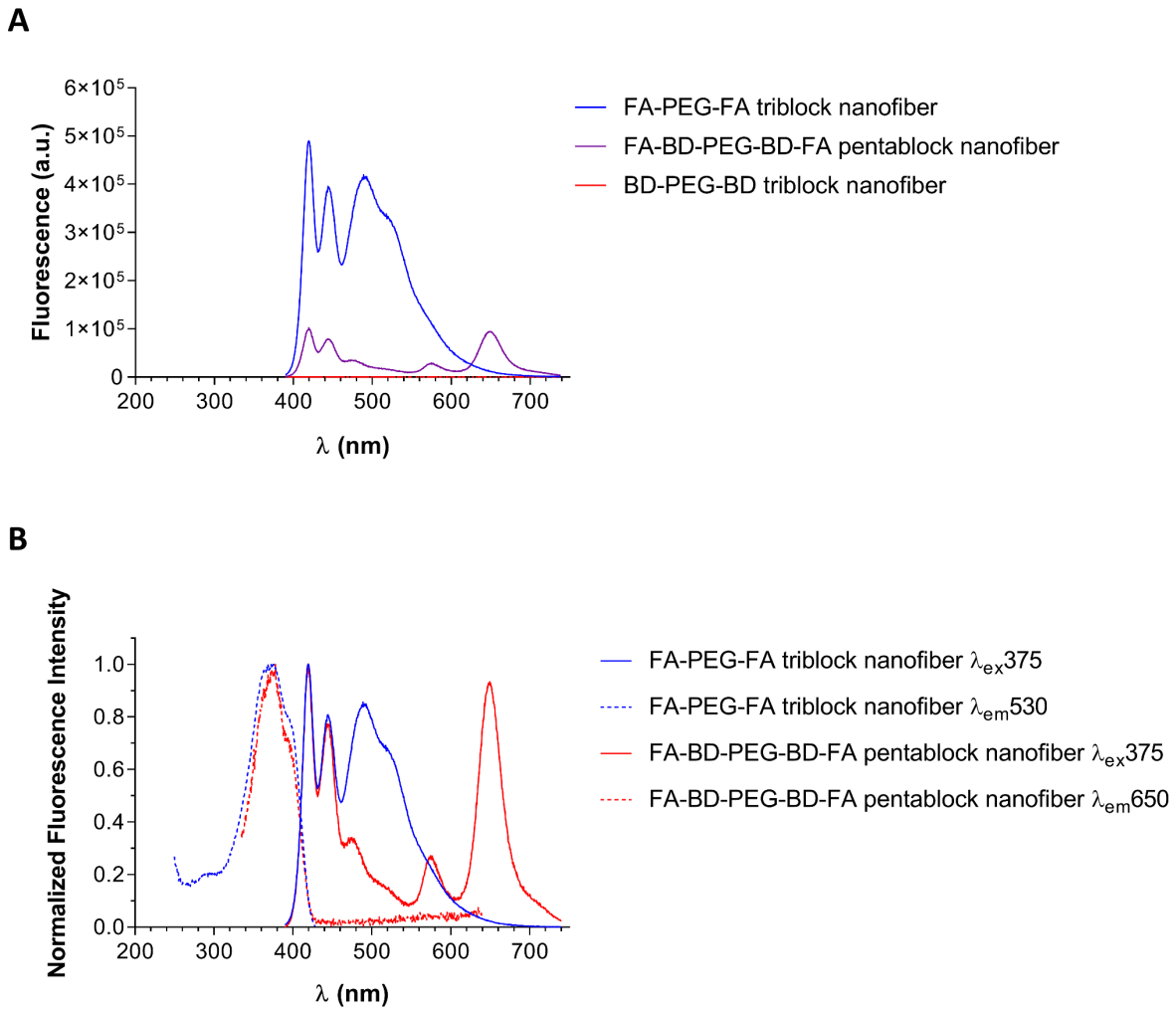

Figure S12. Comparison of fluorescence spectra of $PDHF_{13}$-*b*-PEG_{227} nanofibers in H_2O. (A), Relative fluorescence intensities of the three different micelle systems studied at 50 µg/mL (λ_{ex} = 375 nm). As the concentration of BD increases (FA-PEG-FA>FA-BD-PEG-BD-FA>BD-PEG-BD), the observed fluorescence is increasingly quenched. (B) Overlay of the fluorescence profiles of FA-PEG-FA triblock nanofibers and FA-BD-PEG-BD-FA pentablock nanofibers at 50 µg/mL, highlighting the quenching/blue shift of the longer wavelength emission from PDHF associated with excimer formation[12] and/or keto defects,[13] and the appearance of an emission band corresponding to BD upon excitation of the PDHF core when BD is present. The legend for excitation and emission profiles follows the convention used in Figure S10.

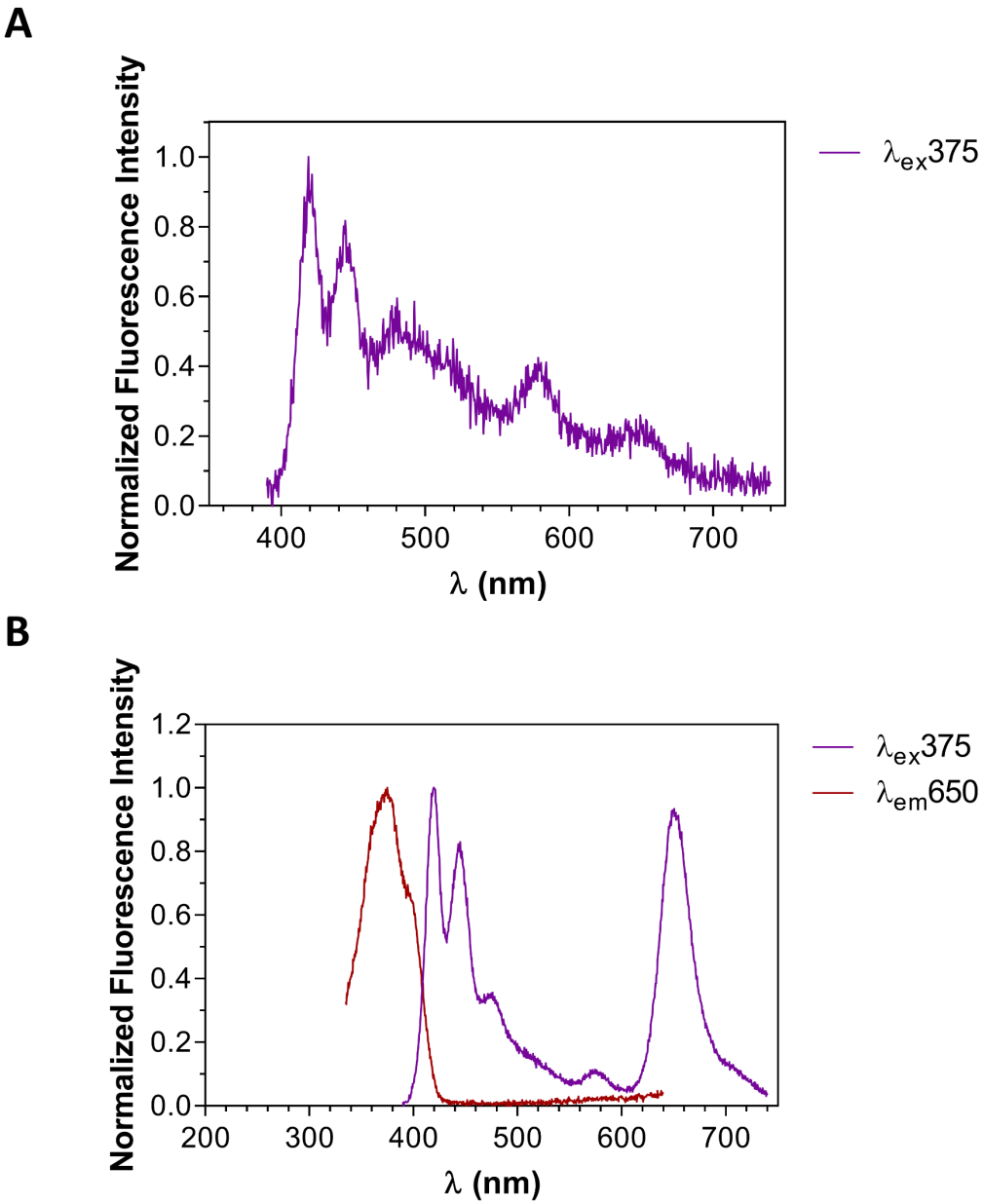

Figure S13. Fluorescence spectra of $PDHF_{13}$-*b*-PEG_{227} nanofibers in PBS. (A) BD-PEG-BD triblock nanofibers (50 µg/mL), and (B) FA-BD-PEG-BD-FA pentablock nanofibers (50 µg/mL). Note the appearance of a detectable emission at 50 µg/mL for BD-PEG-BD triblock nanofibers (versus no detectable emission in pure water in Figure S12). Also note the persistence of the FRET interaction between the BD dye and the PDHF core for both samples, indicating the stability of this interaction under buffered conditions. The legend for excitation and emission profiles follows the convention used in Figure S10.

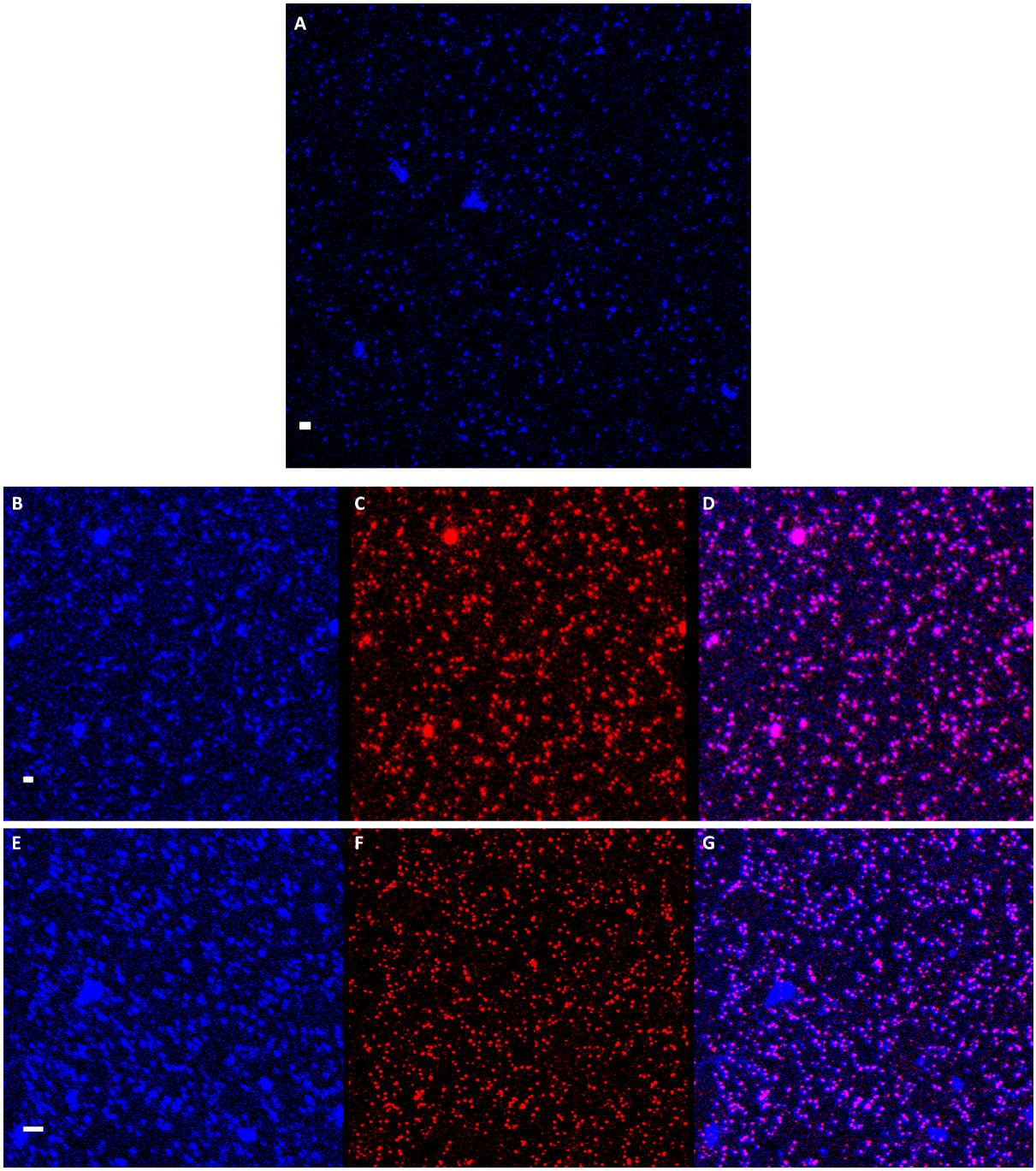

Figure S14. CLSM images of $PDHF_{13}$-*b*-PEG_{227} nanofibers in PBS and cell media. (A) FA-PEG-FA triblock nanofibers (L_n = 90 nm, L_w/L_n = 1.11, σ = 30 nm) in PBS at 100 µg/mL. (B-D) BD-PEG-BD triblock nanofibers (L_n = 85 nm, L_w/L_n = 1.19, σ = 38 nm) in MEM cell media at 100 µg/mL. (E-G) FA-BD-PEG-BD-FA pentablock nanofibers (L_n = 95 nm, L_w/L_n = 1.17, σ = 38 nm) in MEM cell media at 100 µg/mL. (A,B,E) PDHF fluorescence (λ_{ex} = 405 nm, λ_{em} = 415-478 nm). (C,F) BD fluorescence (λ_{ex} = 633 nm, λ_{em} = 640-700 nm). (D,G) Overlay of images B-C & E-F. Scale bars are 2 µm.

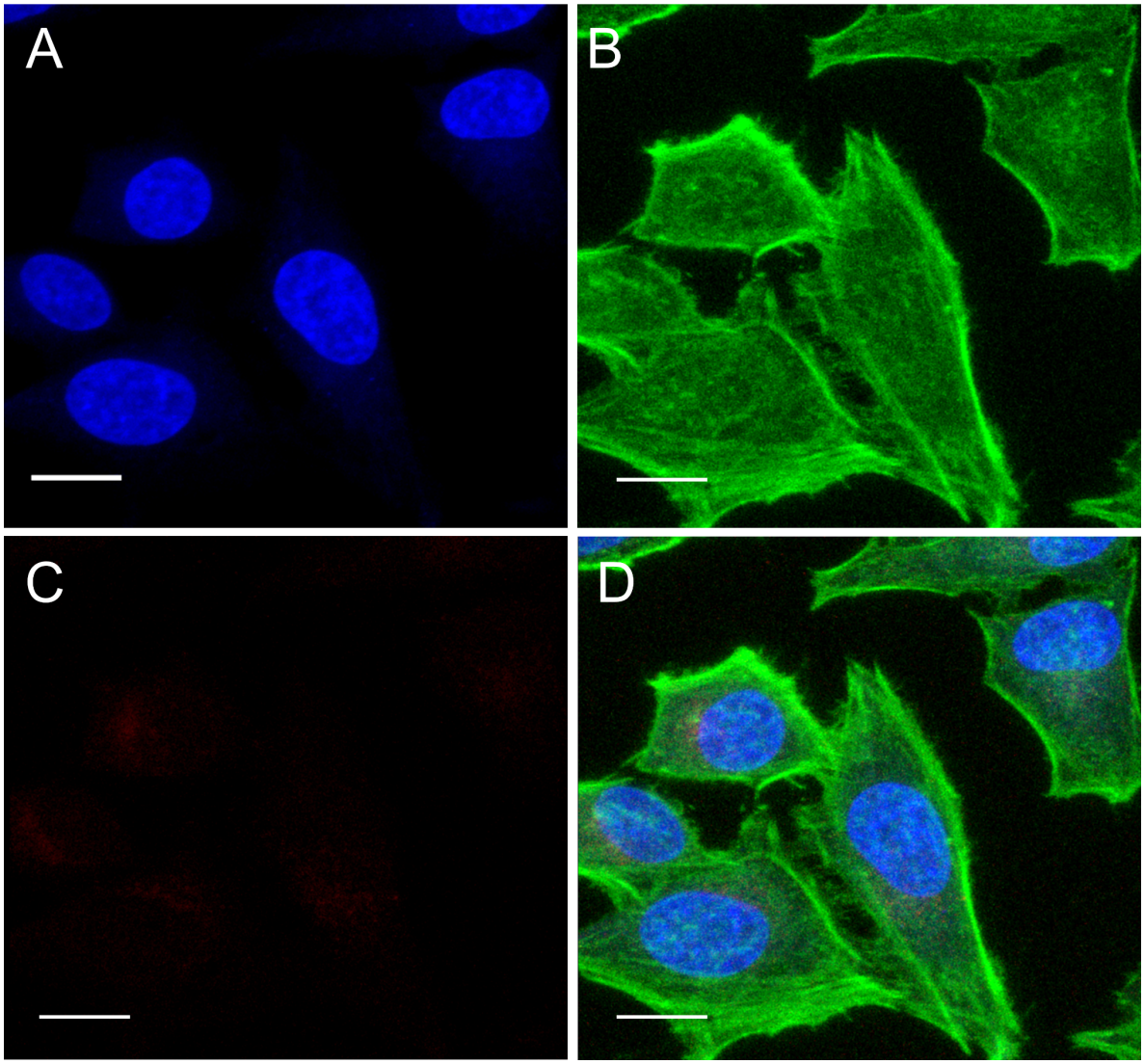

Figure S15. CLSM z-stack of fixed HeLa cells after 1 h exposure to BD-PEG-BD triblock nanofibers (50 µg/mL) reveals limited cellular internalization was observed. (A) Nucleus stained with DAPI. (B) F-Actin stained with Alexa Fluor 488 Phalloidin. (C) Limited fluorescence was observable from BD-PEG-BD triblock nanofibers (λ_{ex} = 633 nm, λ_{em} = 640-700 nm). (D) Overlay of images B-D. Scale bars correspond to 20 µm.

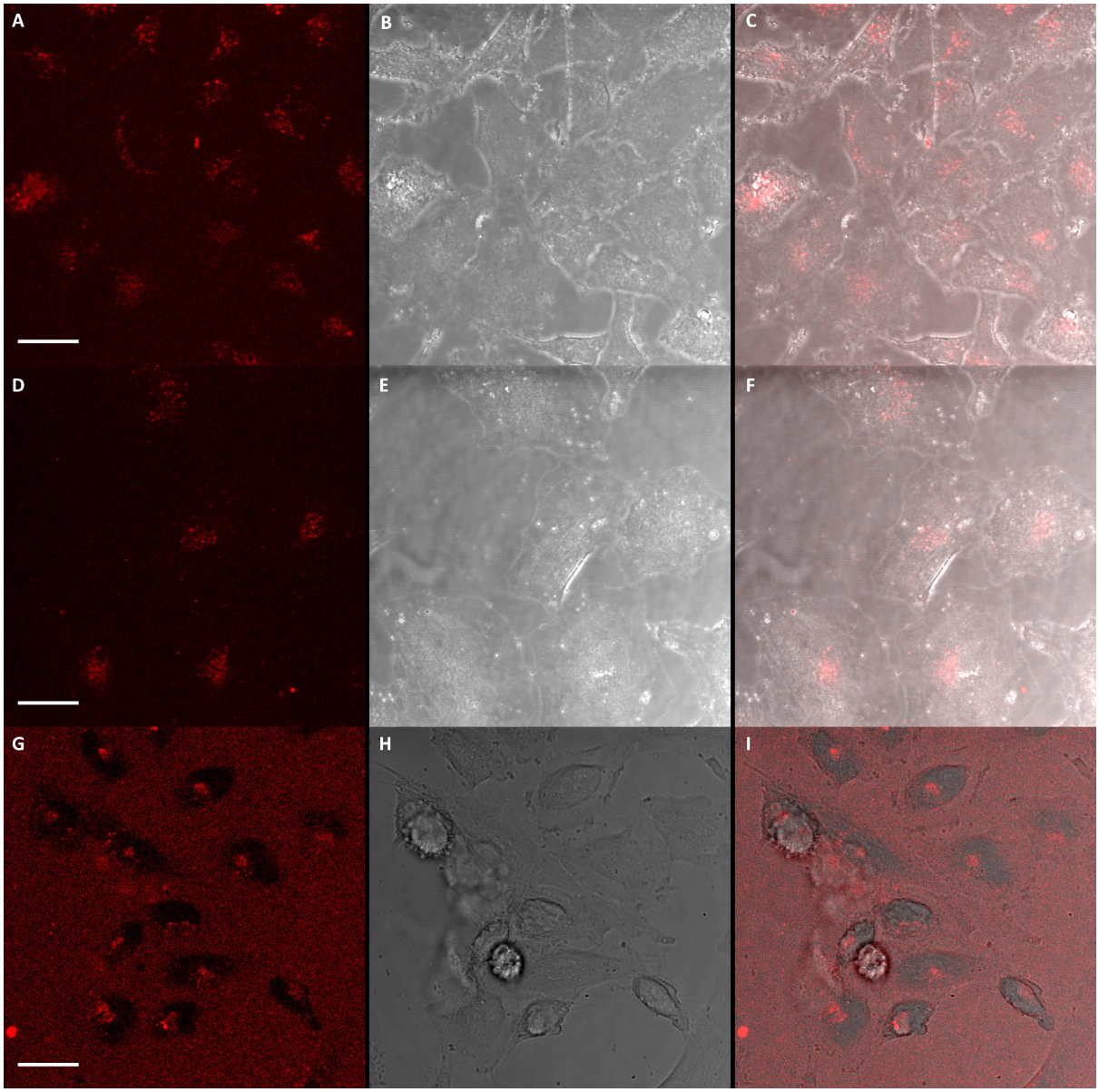

Figure S16. Confocal Laser Scanning Microscopy images of live HeLa cells after 45 minutes exposure to BD-PEG-BD triblock nanofibers (50 μg/mL, L_n = 85 nm, L_w/L_n = 1.19, σ = 38 nm). (A-C) Control HeLa cells. (D-F) HeLa cells exposed to BD-PEG-BD triblock nanofibers. (G-I) HeLa cells exposed to BD-PEG-BD triblock nanofibers, imaged with the supernatant left in solution. The dark spots correspond to cells. (A,D,G) BD fluorescence (λ_{ex} = 633 nm, λ_{em} = 640-700 nm). (B,E,H) brightfield transmitted light channel. (C,F,I) Overlay of images A-B,D-E & G-H. Together, these images show that BD-PEG-BD triblock nanofibers exhibit little uptake by cells within the timeframe of the experiment. Scale bars are 20 μm.

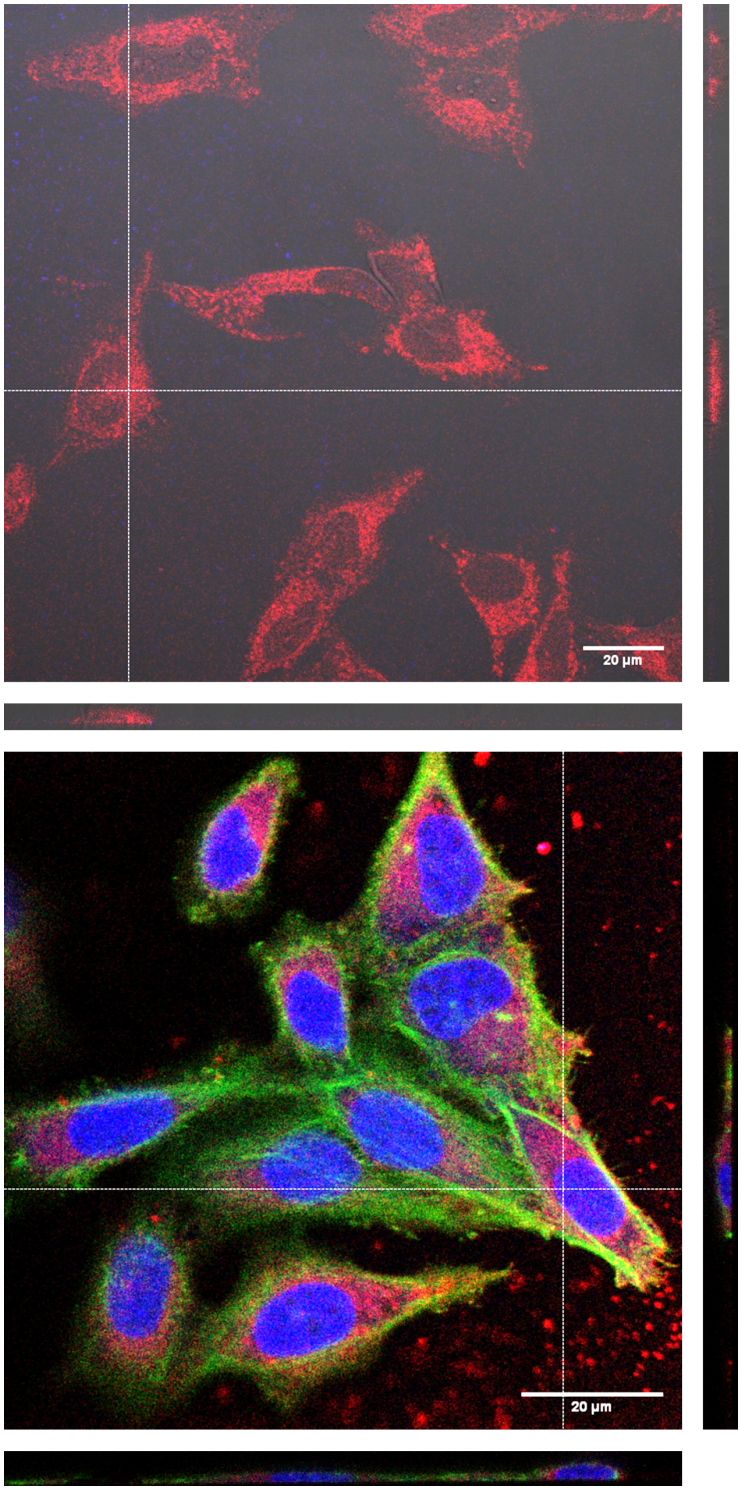

Figure S17. CLSM z-slice and orthogonal sections of live HeLa cells after 30 min exposure to FA-BD-PEG-BD-FA pentablock nanofibers (10 µg/mL, L_n = 95 nm, L_w/L_n = 1.17, σ = 39 nm). The orthogonal sections (smaller bars on x and y axis, plotted from the white dotted lines) show that fluorescence is found throughout the cell, but not within the nucleus (nucleus stained blue with DAPI, F-actin stained green with Alexa Fluor 488-Phalloidin, BD fluorescence in red).

Table S1. Representative flow cytometry results for the uptake of BD-PEG-BD triblock nanofibers (L_n = 85 nm, L_w/L_n = 1.19, σ = 38 nm) or FA-BD-PEG-BD-FA pentablock nanofibers (L_n = 95 nm, L_w/L_n = 1.17, σ = 39 nm) into HeLa cells after a 45 minute incubation.

Sample	Control	Fibers without folic acid	Fibers with folic acid
Cells counted	12,573	12,855	12,416
Cells (%)	88.3	87.9	89.0
Single cells (%)	97.9	97.5	98.3
Live cells (%)	96.9	96.3	96.7
$BODIPY^{630/650\text{-}X}$ positive cells (%)	0.17	0.19	99.7
Median fluorescence intensity of $BODIPY^{630/650\text{-}X}$ (a.u.)	306	483	4,887
Median fluorescence intensity of $BODIPY^{630/650\text{-}X}$ (% control)	100	149	1,664
σ of $BODIPY^{630/650\text{-}X}$ fluorescence (a.u.)	154	219	2,395
Coefficient of variation (a.u.) of $BODIPY^{630/650\text{-}X}$ fluorescence	50.4	45.3	49.0
Geometric mean of $BODIPY^{630/650\text{-}X}$ fluorescence (a.u.)	381	573	4459
PDHF positive cells (%)[a]	0.05	0.02	0.02
σ of PDHF fluorescence	721	713	693
Median fluorescence intensity of PDHF (a.u.)	2,010	2,040	2,010
Median fluorescence intensity of PDHF (% control)	100	105	105
Median Side Scatter Area	40,128	40,704	42,240
σ of Side Scatter Area	15,136	15,392	15,104

[a] PDHF is thought to undergo fluorescence quenching when inside cells.

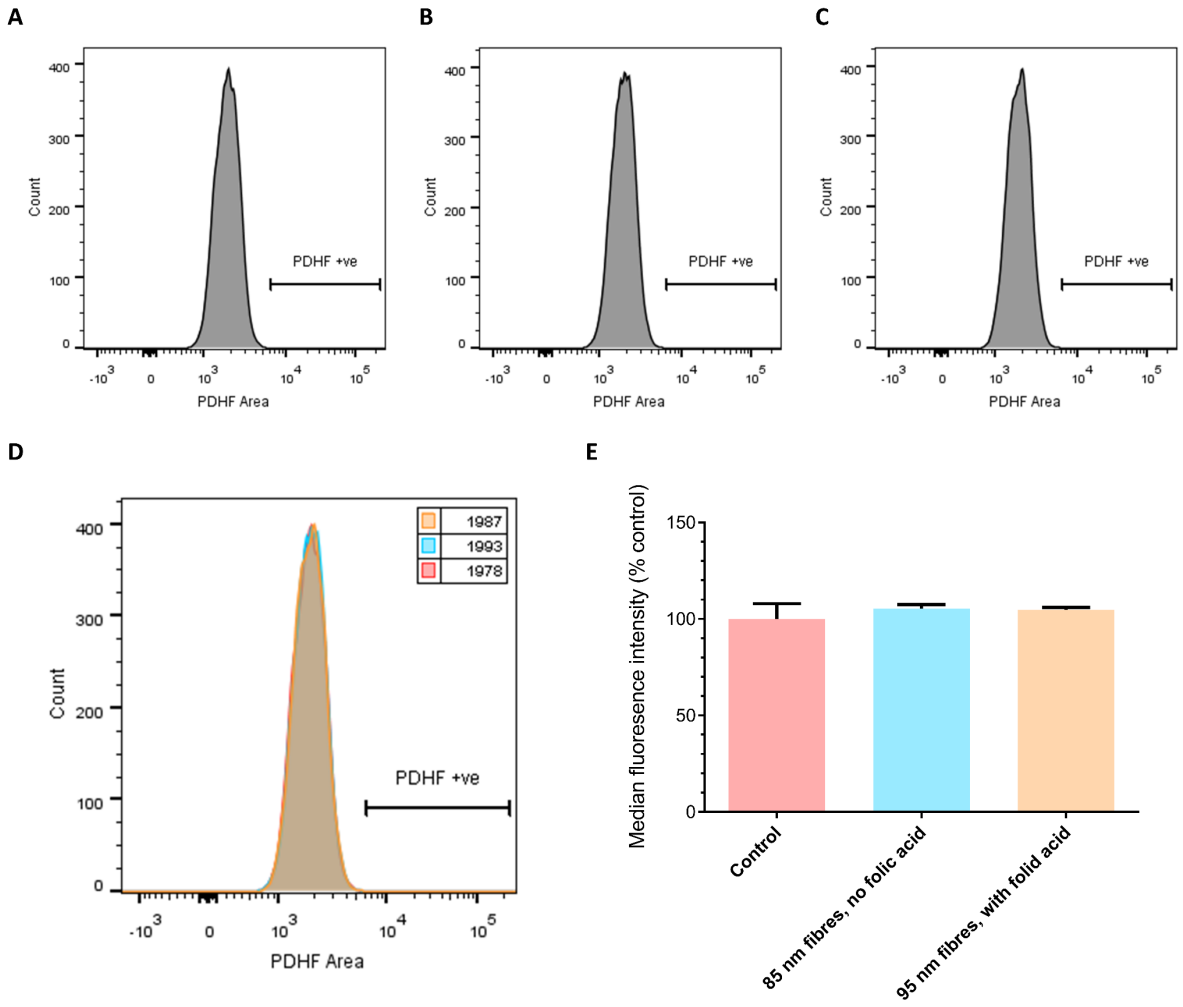

Figure S18. Representative flow cytometry results for the analysis of PDHF fluorescence inside HeLa cells after 45 minutes incubation time (10 µg/mL). (A) Control HeLa cells. (B) BD-PEG-BD triblock nanofibers (C) FA-BD-PEG-BD-FA pentablock nanofibers (D) Overlay of PDHF fluorescence for control cells (red), fibers without folic acid (blue) and fibers with folic acid (yellow), indicating no detectable PDHF fluorescence. *Inset*: geometric mean of PDHF fluorescence channel. (E) Normalized median fluorescence intensity (expressed as % of control) of fibers with/without folic acid and control cells. In all cases, the median fluorescence intensity was no different from control cells.

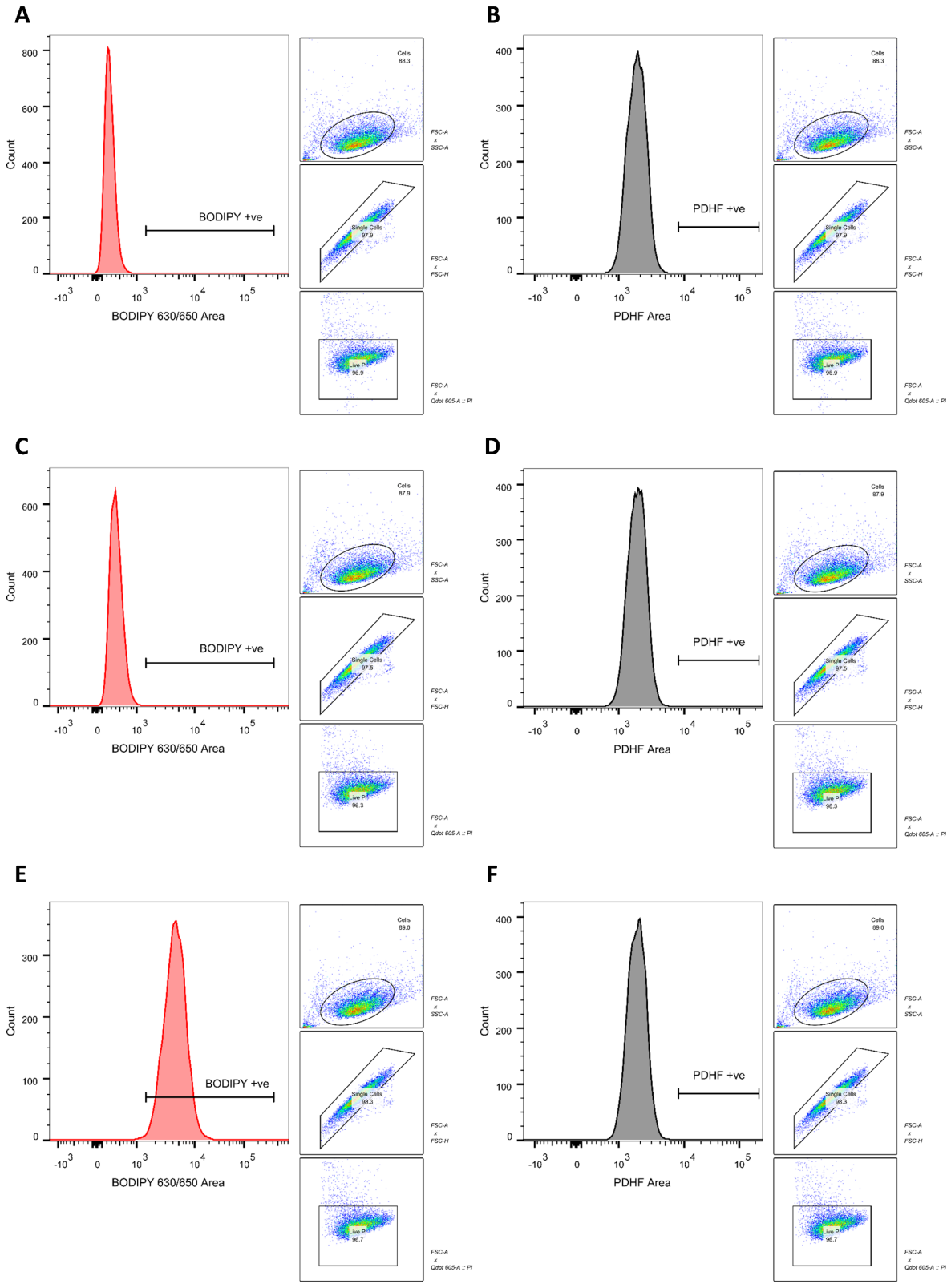

Figure S19. Representative flow cytometry results with gating ancestry for (A,C,E) BD fluorescence and (B,D,F) PDHF fluorescence. (A-B) Control HeLa cells. (C-D) BD-PEG-BD triblock nanofibers (E-F) FA-BD-PEG-BD-FA pentablock nanofibers. Both nanofibers were incubated with cells for 45 minutes before counting.

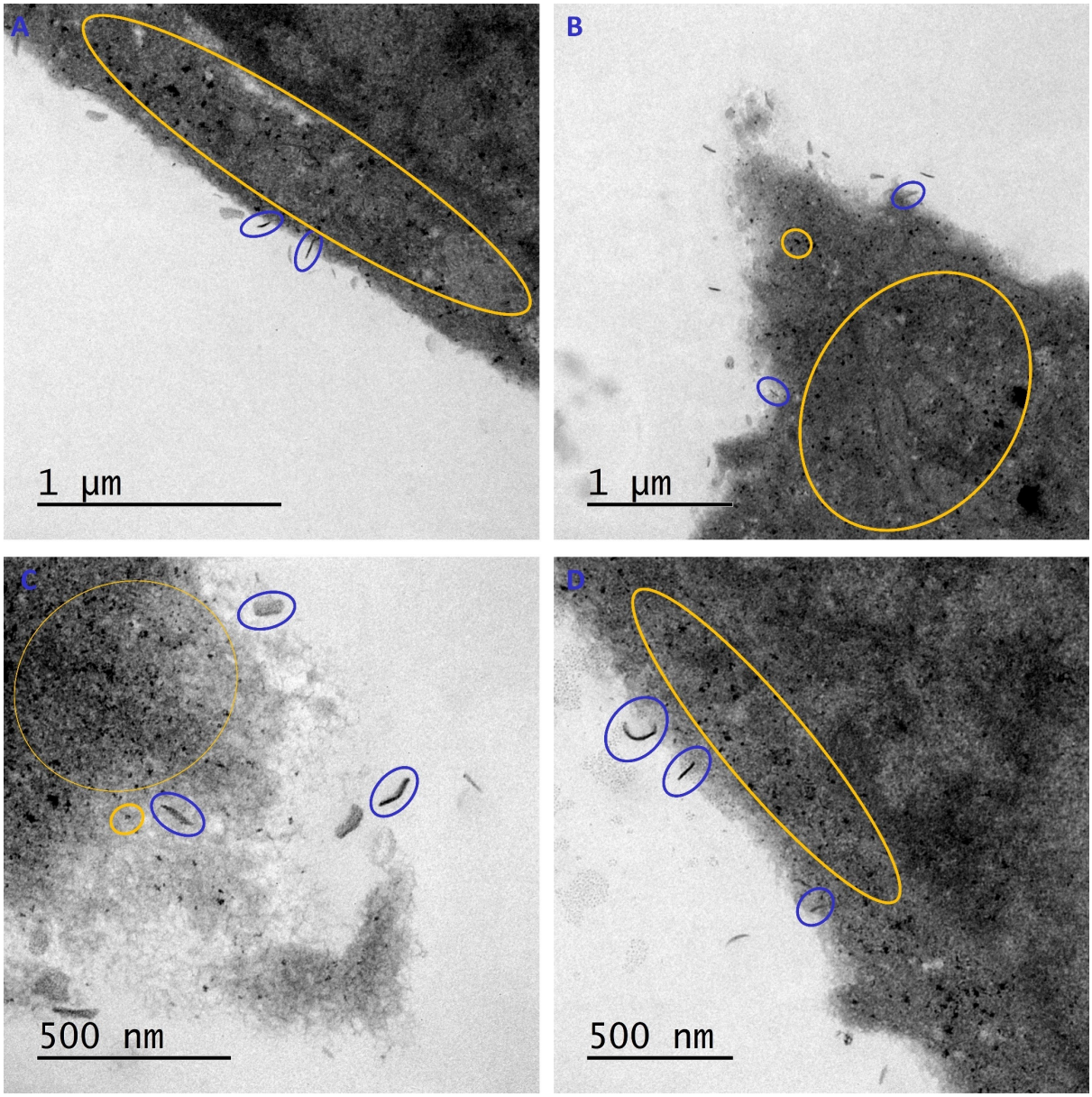

Figure S20. Further TEM micrographs of FA-BD-PEG-BD-FA pentablock nanofibers interacting with the cell membrane of HeLa cells expressing GRASP65-GFP after 10 minutes incubation at 4 °C. Note the significant number of nanofibers interacting in an end-on fashion (blue circles), as well as nanofibers which appear to be disassembling (e.g. in image C) and appear to be breaking up into smaller fragments (which are highlighted in the yellow circles), inside a cloud of less electron-dense material. Furthermore, note the electron-dense fragments observed around the outer layer of the cell which are not present further in (e.g. in image D).

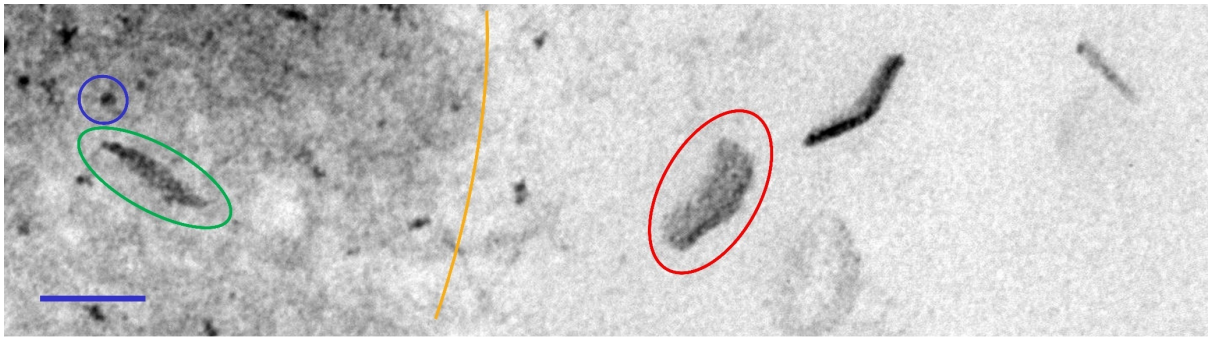

Figure S21. Magnified TEM micrograph of FA-BD-PEG-BD-FA pentablock nanofibers interacting with the cell membrane of HeLa cells expressing GRASP65-GFP after 10 minutes incubation at 4 °C. The contour of the cell membrane is highlighted in yellow. Note the association of the nanofibers with an unknown species (less electron-dense cloud surrounding the nanofibers, circled in red), and what appears to be disassembly of the nanofiber in the fiber circled in green, which matches the small electron dense fragments observed around the edges of the cell (also visible, circled in blue). Scale bar = 100 nm.

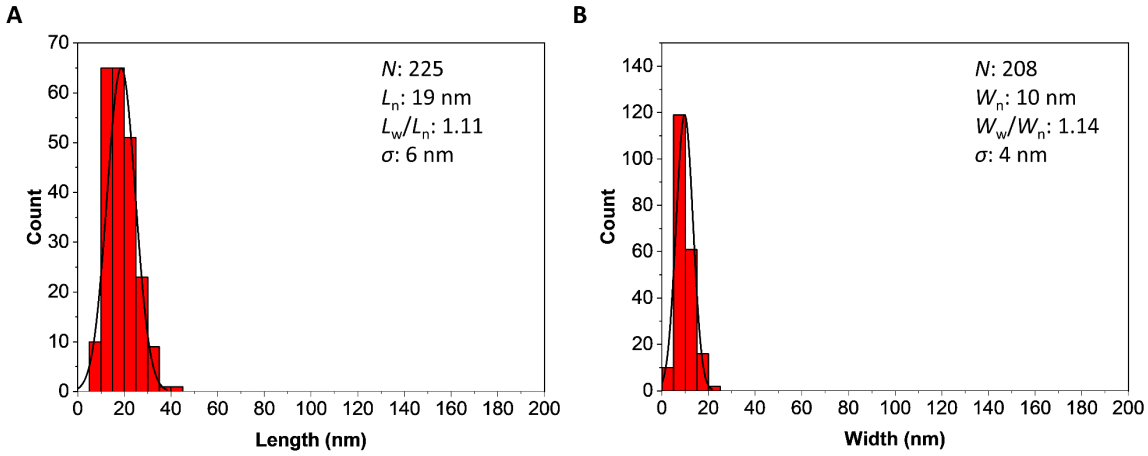

Figure S22. Analysis of the length and width of anisotropic fragments observed inside cells via TEM. Histograms of (A) length and (B) width of HeLa cells expressing GRASP65-GFP exposed to FA-BD-PEG-BD-FA pentablock nanofibers (50 μg/mL) after 90 minutes incubation. Note that the widths of the particles are consistent with those expected for $PDHF_{13}$-*b*-PEG_{227} nanofibers.[11] A minimum of 200 particles was counted in each case.

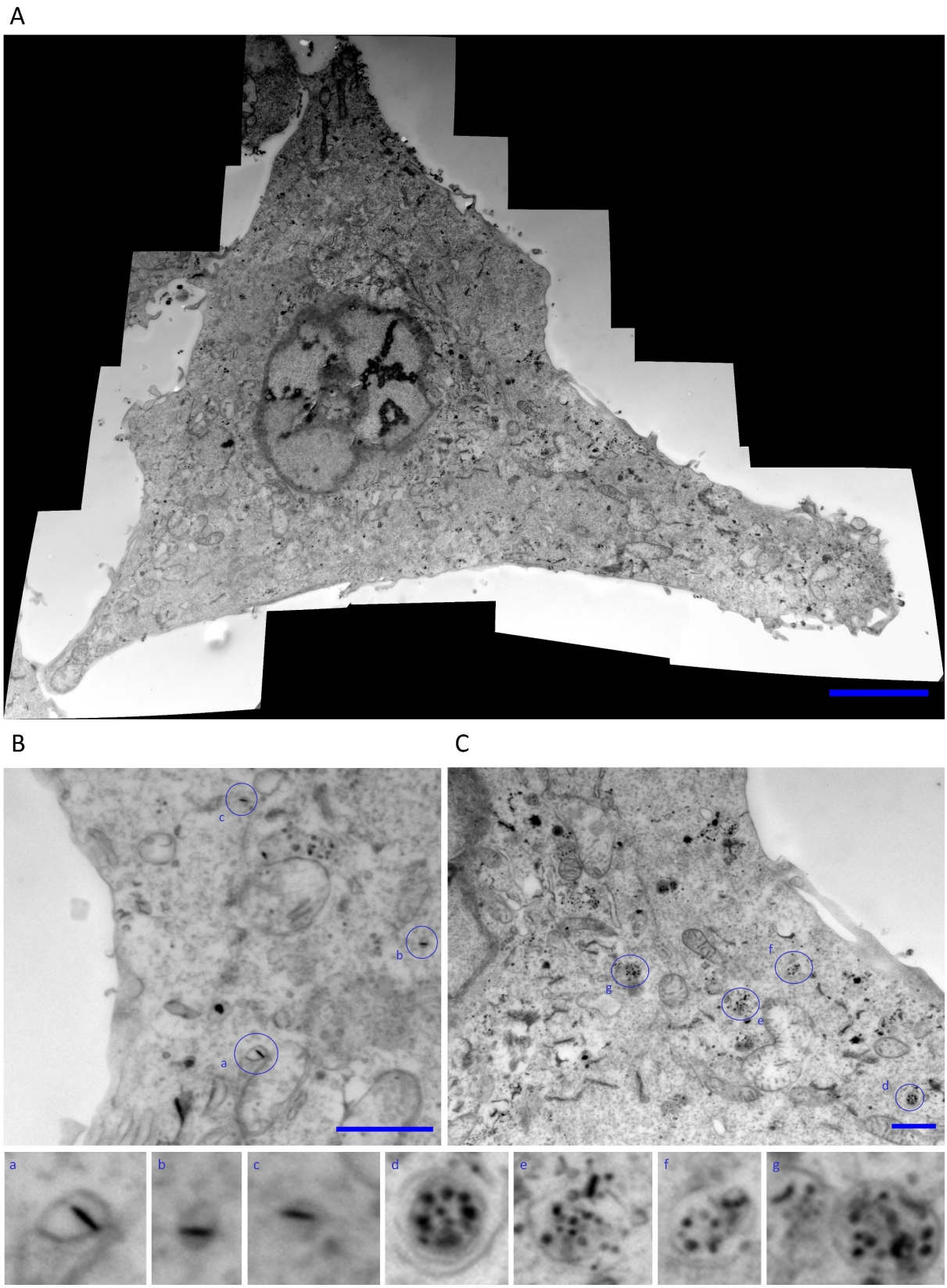

Figure S23. (A) High-resolution composite TEM micrograph of a single cell following 10 min incubation at 4 °C with FA-BD-PEG-BD-FA pentablock nanofibers (50 μg/mL, L_n = 95 nm, L_w/L_n = 1.17, σ = 39 nm). The composite TEM micrograph has been stitched together from 16

individual images, using Microsoft ICE 2.0 (Microsoft Corporation). (B) Magnified image highlighting intact nanofibers inside endosomes (circled blue, magnified in a-c). (C) Magnified image highlighting endosomes / lysosomes with nanofiber fragments inside (circled blue, magnified in d-g). Scale is 5 µm for A, and 1 µm for B-C.

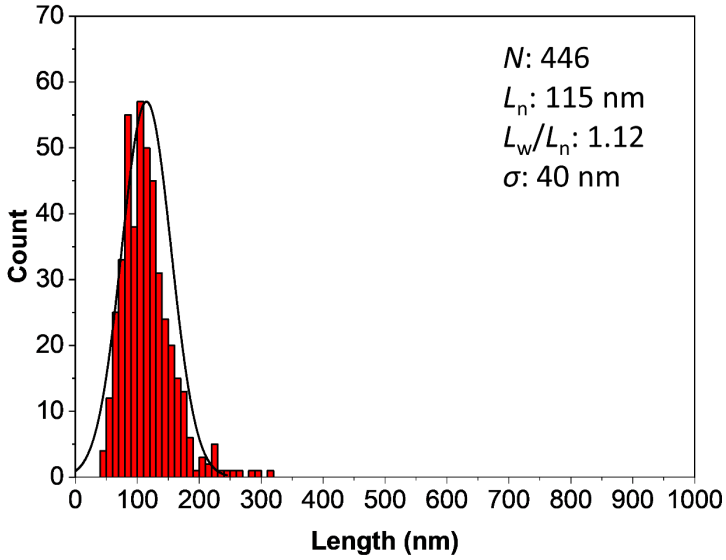

Figure S24. Histogram of the length of intact FA-BD-PEG-BD-FA pentablock nanofibers observed inside a single GRASP65-GFP HeLa cell (Figure S23A) following 10 min incubation at 4 °C with FA-BD-PEG-BD-FA pentablock nanofibers (50 µg/mL, L_n = 95 nm, L_w/L_n = 1.17, σ = 39 nm). Bin size is 10 nm.

Table S2. Summary of the statistical measurements of the length of intact nanofibers observed inside a single GRASP65-GFP HeLa cell (Figure S23A) following 10 min incubation at 4 °C with FA-BD-PEG-BD-FA pentablock nanofibers (50 µg/mL, L_n = 95 nm, L_w/L_n = 1.17, σ = 39 nm).

N	446
L_n (nm)	115
σ (nm)	40
σ / L_n (nm)	0.348
L_w (nm)	129
L_w / L_n	1.12

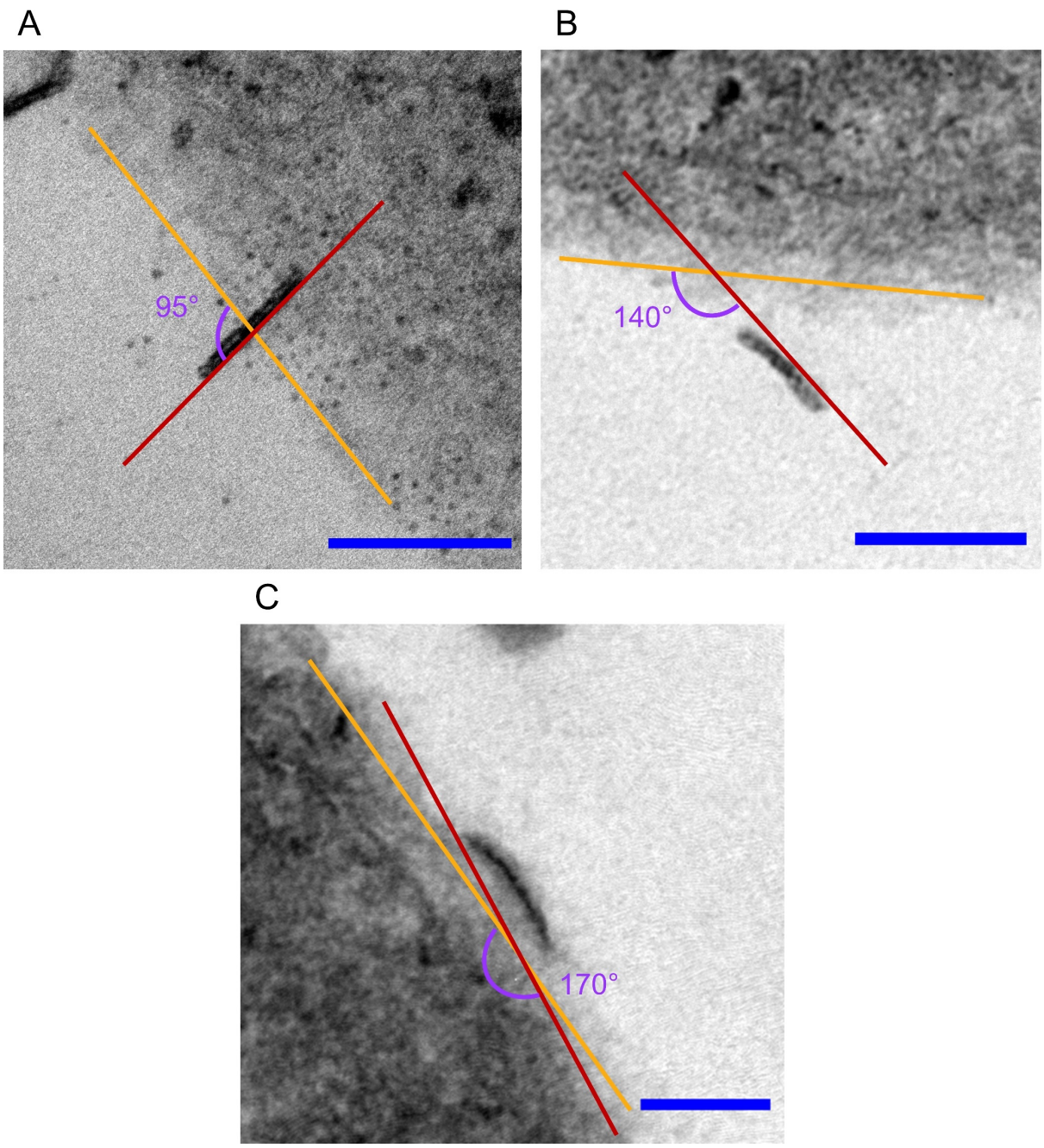

Figure S25. Representative examples of entry angle measurements for FA-BD-PEG-BD-FA pentablock nanofibers observed entering GRASP65-GFP HeLa cells. The yellow lines represent the estimated cell contour, the red lines represent the estimated nanofiber contour, and the purple lines represent the angle measured. (A) 95° entry angle. (B) 140° entry angle. (C) 170° entry angle. Scale bars = 100 nm.

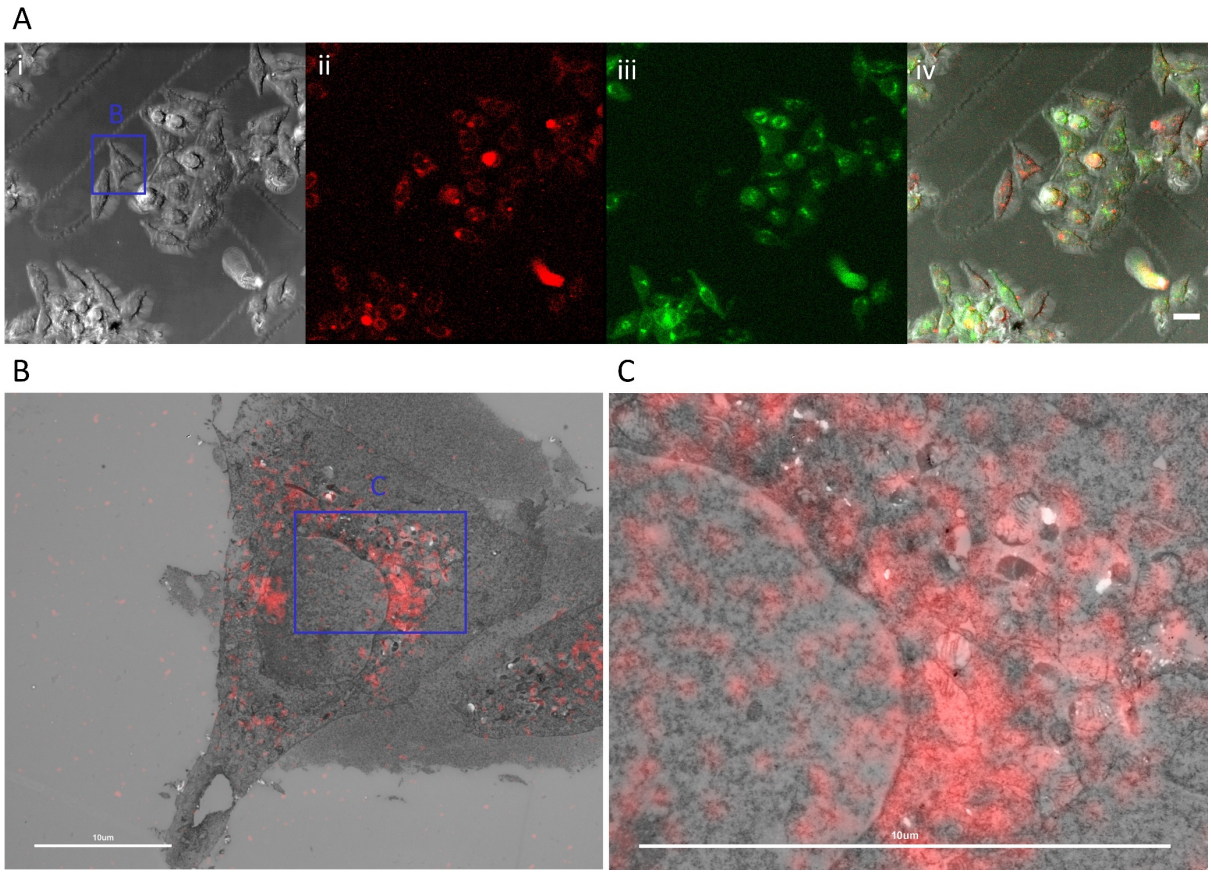

Figure S26. CLEM studies on HeLa cells expressing GRASP65-GFP incubated with 95 nm FA-BD-PEG-BD-FA pentablock nanofibers for 90 min at 22 °C (after association at 4 °C). (A) CLSM images used to produce the overlaid CLEM images. (i) brightfield transmitted light channel, with the cell used in B highlighted. (ii) red channel from BD fluorescence (λ_{ex} = 633 nm, λ_{em} = 640-700 nm). (iii) fluorescence from GRASP65-GFP labelled Golgi Apparatus. (iv) overlay of i-iii. (B) Overlay of z-projection CLSM and TEM images of a single cell, illustrating the fluorescence correlated to the perinuclear region. (C) High magnification overlaid CLSM and TEM image of the section highlighted in B, with the fluorescence emission from CLSM observed around the perinuclear region, which corresponds to the location of a high density of electron dense particles thought to be FA-BD-PEG-BD-FA pentablock nanofiber fragments. Scale bars are 20 µm for A and 10 µm for B-C.

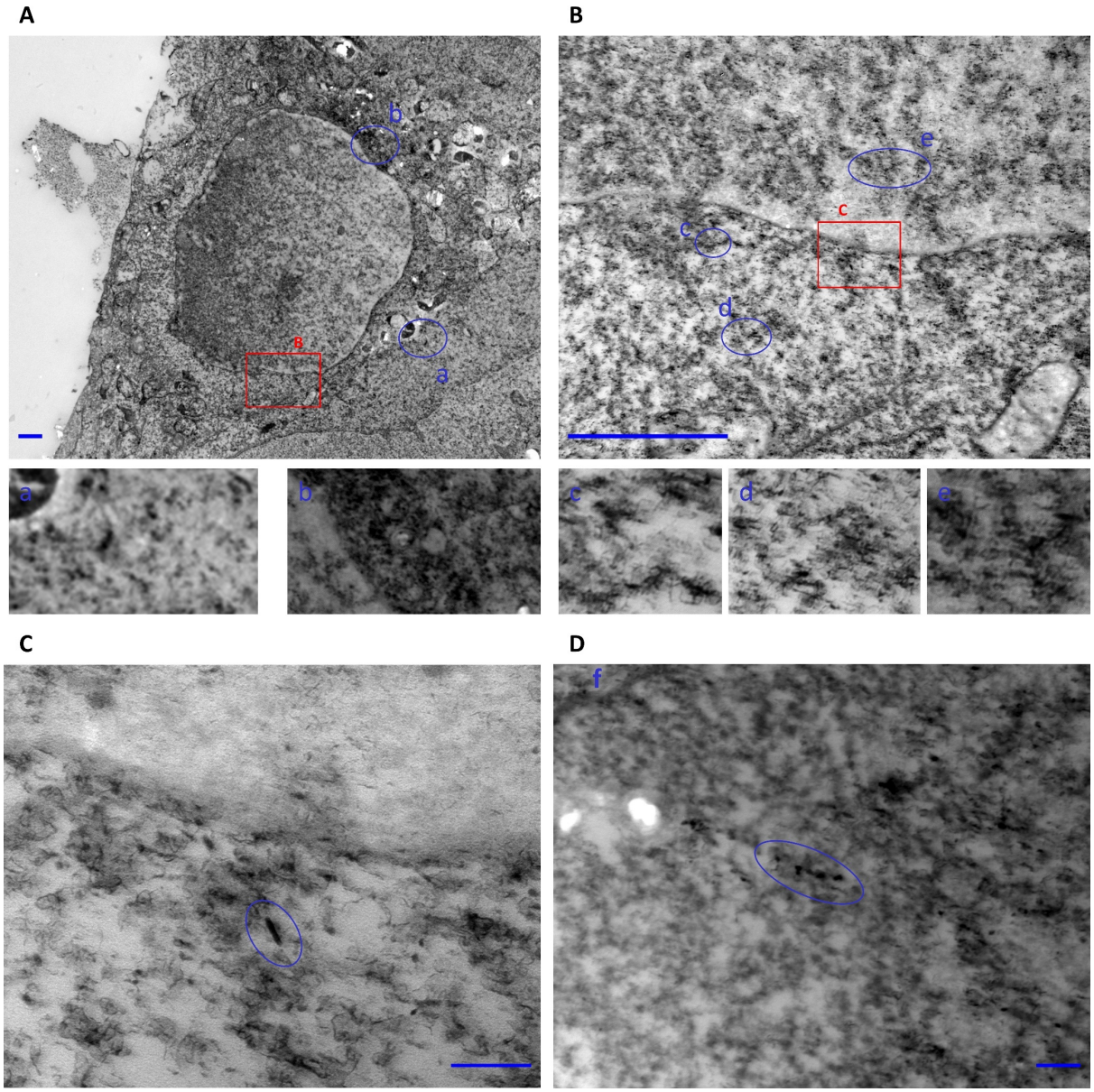

Figure S27. Representative TEM micrographs from HeLa cells expressing GRASP65-GFP exposed to FA-BD-PEG-BD-FA pentablock nanofibers (50 μg/mL) after 90 minutes incubation (CLEM studies). (A) low magnification image showing an overview of the cell, with the area in B highlighted, and intact nanofibers circled in blue (magnified in a-b). (B) Magnified image of the perinuclear region from A. Note the appearance of electron dense particles (nanofibers and possible fragments) around the nuclear membrane, examples of which are highlighted (magnified in c-e). The area in C is highlighted. (C) The perinuclear region from B, with a nanofiber highlighted. (D) Another TEM micrograph of the perinuclear region, with fragments highlighted. The nucleus is labelled f. Scale bars are 1 μm for A-B, and 100 nm for C-D.

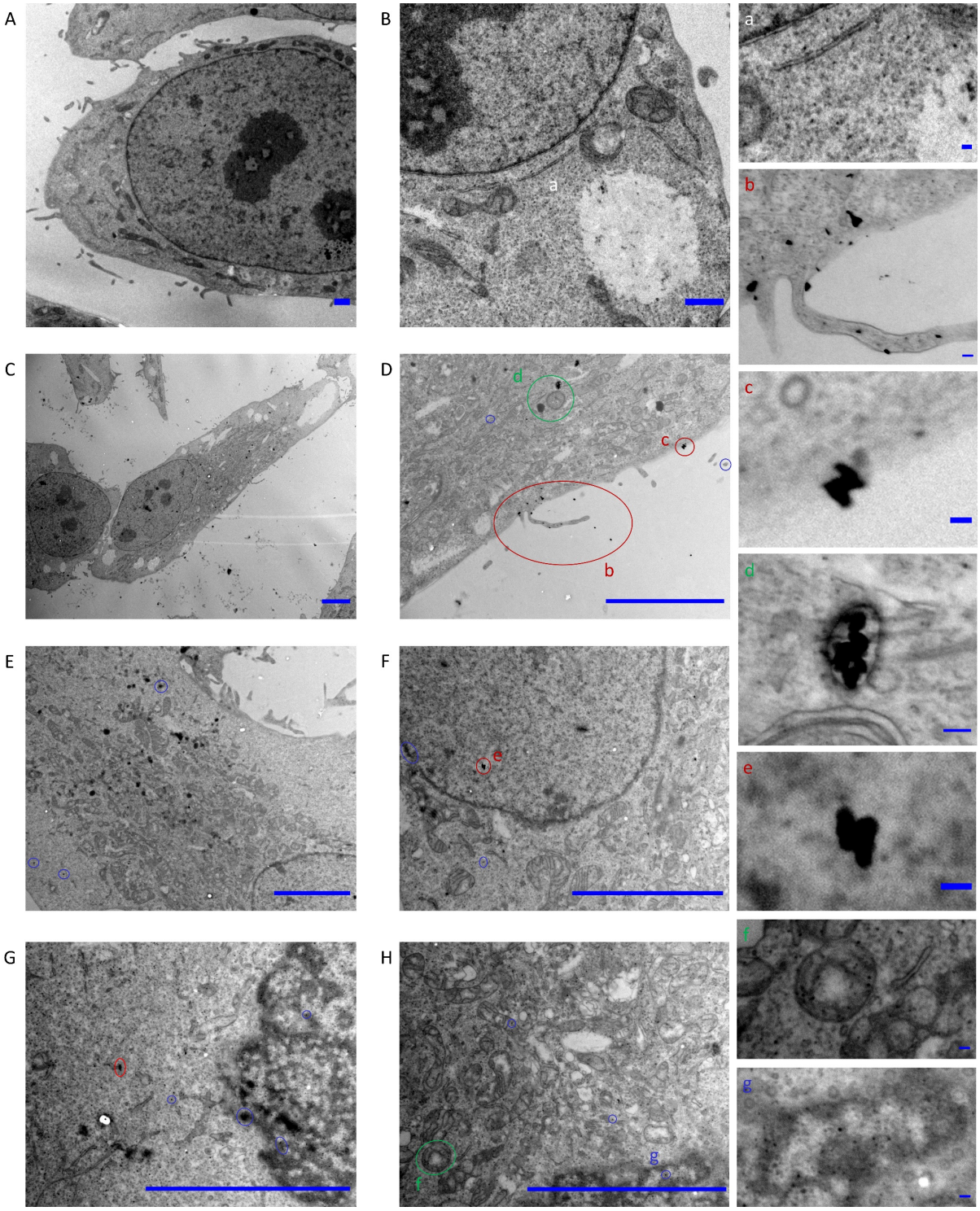

Figure S28. Examples of TEM micrographs from control HeLa cells (A-B) and (C-H) HeLa cells exposed to FA-PEG-FA triblock nanofibers (100 µg/mL, L_n = 90 nm, L_w/L_n = 1.11, σ = 30 nm) after 5 minutes incubation at 37 °C. Note the electron dense particles (possible nanofiber fragments / clusters) around and on the nuclear membrane, endosomes / lysosomes, and intact nanofibers. Magnifications of each labelled feature are in a-g. Scale bars are 5 µm for A-H and 100 nm for a-f.

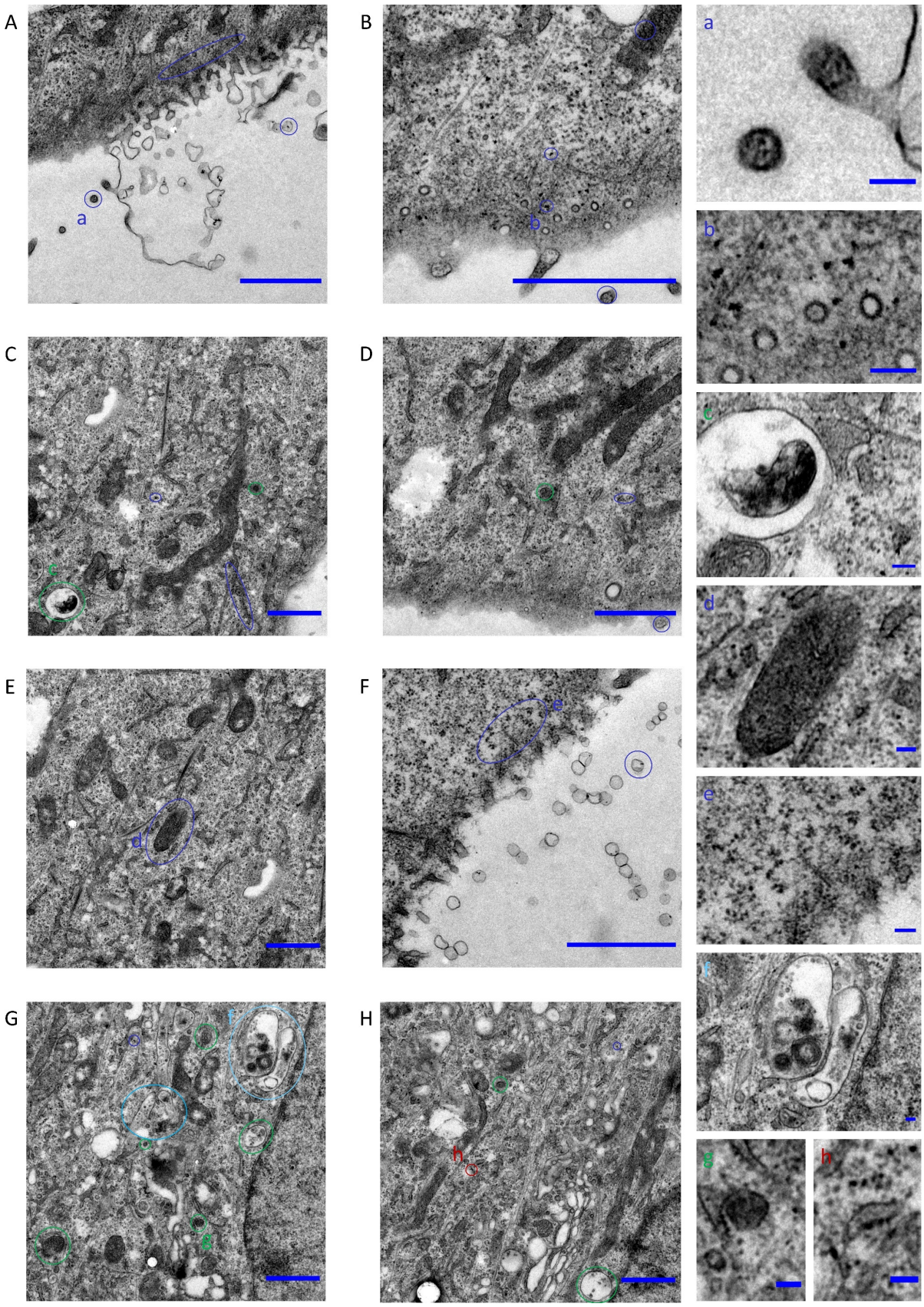

Figure S29. Examples of TEM micrographs from HeLa cells exposed to FA-PEG-FA triblock nanofibers (500 μg/mL, L_n = 90 nm, L_w/L_n = 1.11, σ = 30 nm) after 75 minutes incubation. Note the increase in electron dense particles (possible nanofiber fragments) throughout the cell,

as well as endosomes / lysosomes, including some rupturing endosomes / lysosomes and an intact nanofiber. Magnifications of each labelled feature are in a-h. Scale bars are 1 µm for A-H, and 100 nm for a-h.

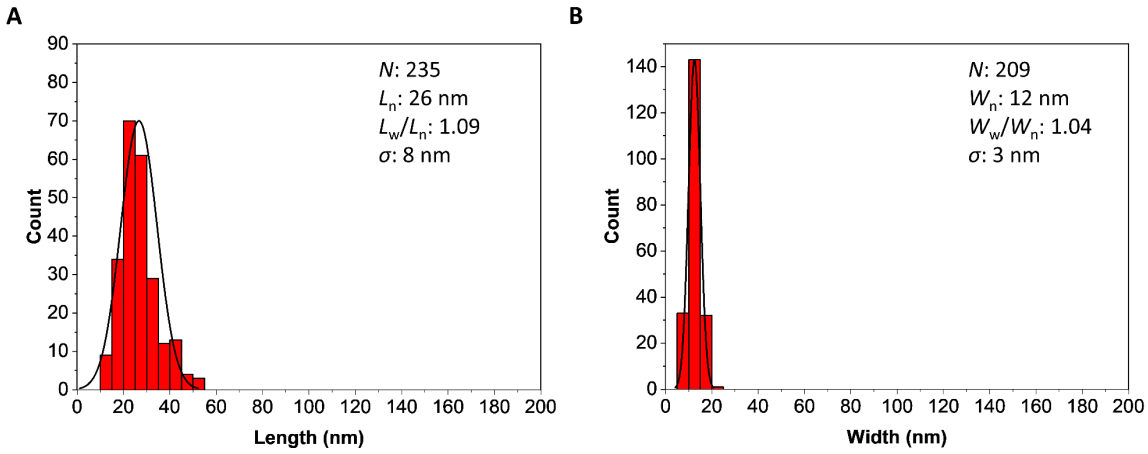

Figure S30. Analysis of the length and width of anisotropic electron dense particles observed via TEM inside HeLa cells exposed to FA-PEG-FA triblock nanofibers (100 µg/mL) after 5 minutes incubation. Histograms of (A) length and (B) width of particles. Note that the widths of the particles are consistent with those expected for $PDHF_{13}$-*b*-PEG_{227} nanofibers.[11] A minimum of 200 particles were counted in each case.

Table S3. Change in reductive metabolism of WI-38 and HeLa cells upon addition of BD-PEG-BD triblock nanofibers (L_n = 85 nm, L_w/L_n = 1.19, σ = 38 nm) as measured by 72 h alamarBlue™ assay. Values are expressed as % of control.

[BD-PEG-BD triblock nanofibers] (μg/mL)		Control	100	75	50	25	10	5	2.5	1	Staurosporine (1 μM /mL)
WI-38	Mean	100	107	106	111	100	97.6	93.9	97.6	89.5	5.4
	σ	19.4	15.7	6.8	5.1	1.4	7.0	4.6	6.9	8.6	7.2
HeLa	Mean	100	93.6	95.6	91.9	95.5	92.0	103	91.4	100	5.6
	σ	12.9	8.4	6.8	10.8	11.6	11.0	13.6	14.7	10.1	2.9

Table S4. Change in reductive metabolism of WI-38 and HeLa cells upon addition of FA-PEG-FA triblock nanofibers (L_n = 90 nm, L_w/L_n = 1.11, σ = 30 nm) as measured by 72 h alamarBlue™ assay. Staurosporine was used as a positive control. Values are expressed as % of control.

[FA-PEG-FA triblock nanofibers] (μg/mL)		Control	100	75	50	25	10	5	2.5	1	Staurosporine (1 μM /mL)
WI-38	Mean	100	85.9	96.6	110	123	111	101	113	112	0.1
	σ	22.7	19.8	3.0	3.4	12.4	6.1	8.7	4.8	11.0	4.7
HeLa	Mean	100	105	104	101	105	101	101	105	111	0.1
	σ	7.1	10.1	4.4	5.2	9.2	5.7	4.8	6.5	7.0	2.4

Table S5. Change in cell viability of WI-38 and HeLa cells upon addition of BD-PEG-BD triblock nanofibers (L_n = 85 nm, L_w/L_n = 1.19, σ = 38 nm) as measured by 72 h calcein assay. Staurosporine was used as a positive control. Values are expressed as % of control.

[BD-PEG-BD triblock nanofibers] (μg/mL)		Control	100	75	50	25	10	5	2.5	1	Staurosporine (1 μM /mL)
WI-38	Mean	100	79.7	96.8	89.1	91.3	89.8	99.8	88.0	99.6	0.6
	σ	8.5	14.4	5.7	9.4	9.9	7.8	15.2	7.0	5.9	0.7
HeLa	Mean	100	93.2	93.8	105	94.3	93.8	99.1	107	105	0.1
	σ	10.1	13.3	12.2	18.5	18.3	23.7	12.3	12.8	13.1	0.3

Table S6. Change in in cell viability of WI-38 and HeLa cells upon addition of FA-PEG-FA triblock nanofibers (L_n = 90 nm, L_w/L_n = 1.11, σ = 30 nm) as measured by 72 h calcein assay. Staurosporine was used as a positive control. Values are expressed as % of control.

[FA-PEG-FA triblock nanofibers] (μg/mL)		Control	100	75	50	25	10	5	2.5	1	Staurosporine (1 μM /mL)
WI-38	Mean	100	96.7	126	108	103	89.2	105	110	116	0.1
	σ	8.6	24.9	10.9	8.4	5.8	4.4	10.0	20.8	7.5	0.3
HeLa	Mean	100	97.8	106	112	114	107	107	123	117	0.5
	σ	10.3	15.2	14.9	22.1	19.2	18.6	27.2	15.4	20.3	0.5

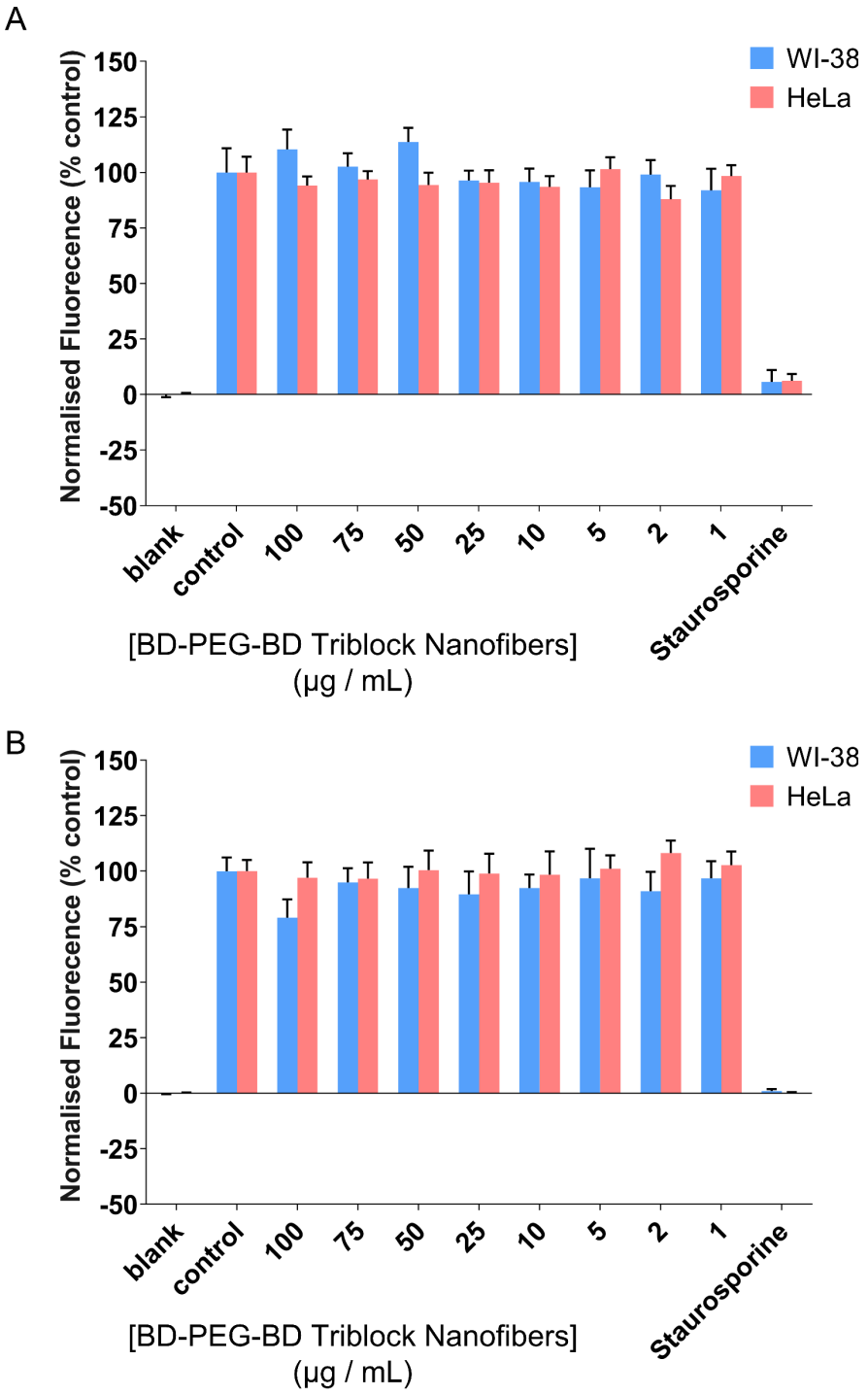

Figure S31. Cytotoxic effects of BD-PEG-BD triblock nanofibers (L_n = 85 nm, L_w/L_n = 1.19, σ_L = 38 nm) upon primary foetal lung fibroblasts (WI-38, light blue), and human cervical adenocarcinoma cells (HeLa, red). Measured after 72 h exposure using (A) alamarBlue™ to assess reductive metabolism or (B) calcein AM to assess live cells. No statistically significant change in cell viability was observed at any nanofiber concentration up to 100 µg/mL for HeLa cells, and up to 75 µg/mL for WI-38 cells. Staurosporine was used as a positive control. Error is represented at a 95 % CI.

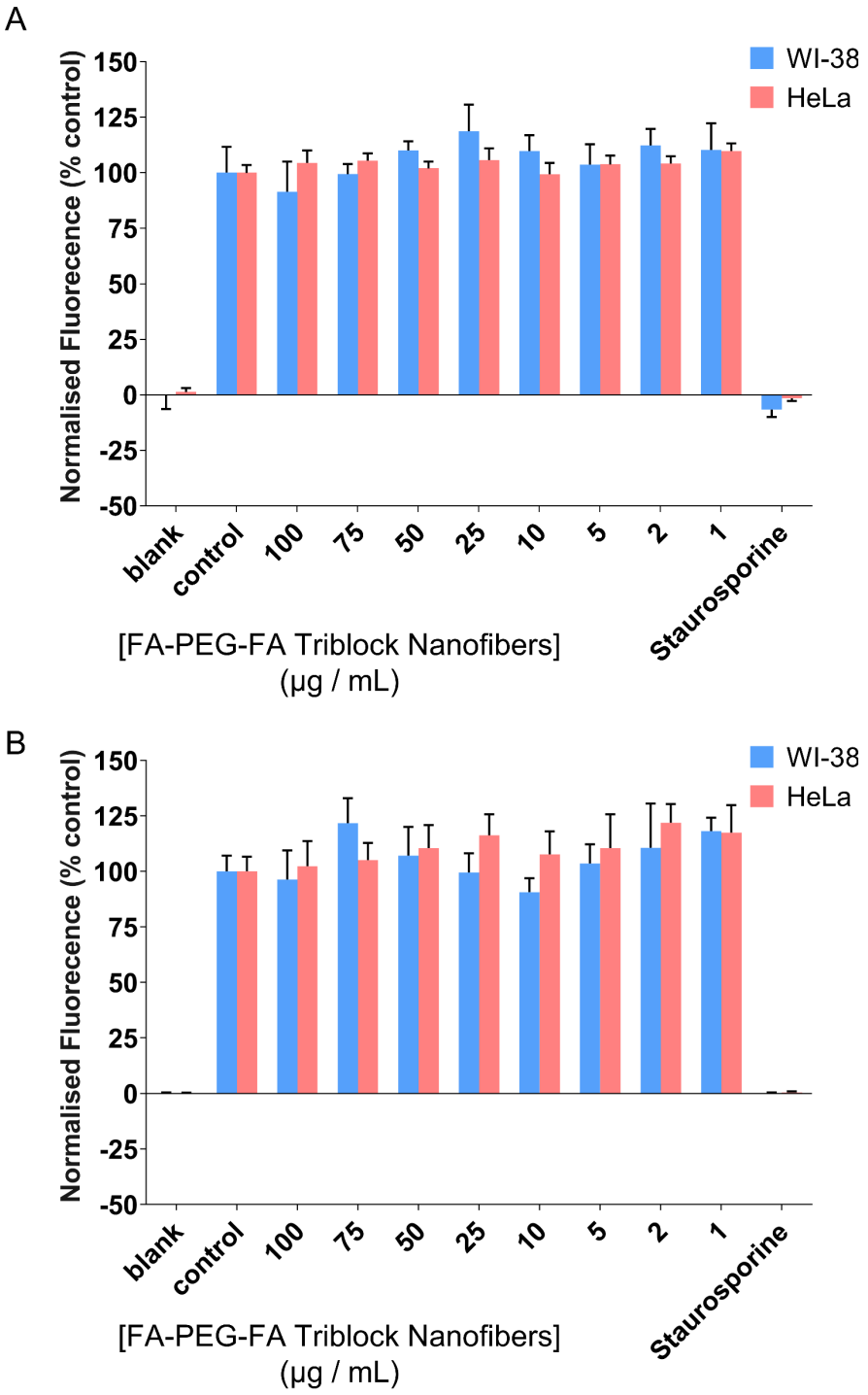

Figure S32. Cytotoxic effects of FA-PEG-FA triblock nanofibers (L_n = 90 nm, L_w/L_n = 1.11, σ = 30 nm) upon primary foetal lung fibroblasts (WI-38, light blue), and human cervical adenocarcinoma cells (HeLa, red). Measured after 72 h exposure using (A) alamarBlue™ to assess reductive metabolism or (B) calcein AM to assess live cells. No statistically significant change in cell viability was observed at any nanofiber concentration up to 100 μg/mL for either WI-38 or HeLa cells. Staurosporine was used as a positive control. Error is represented at a 95 % CI.

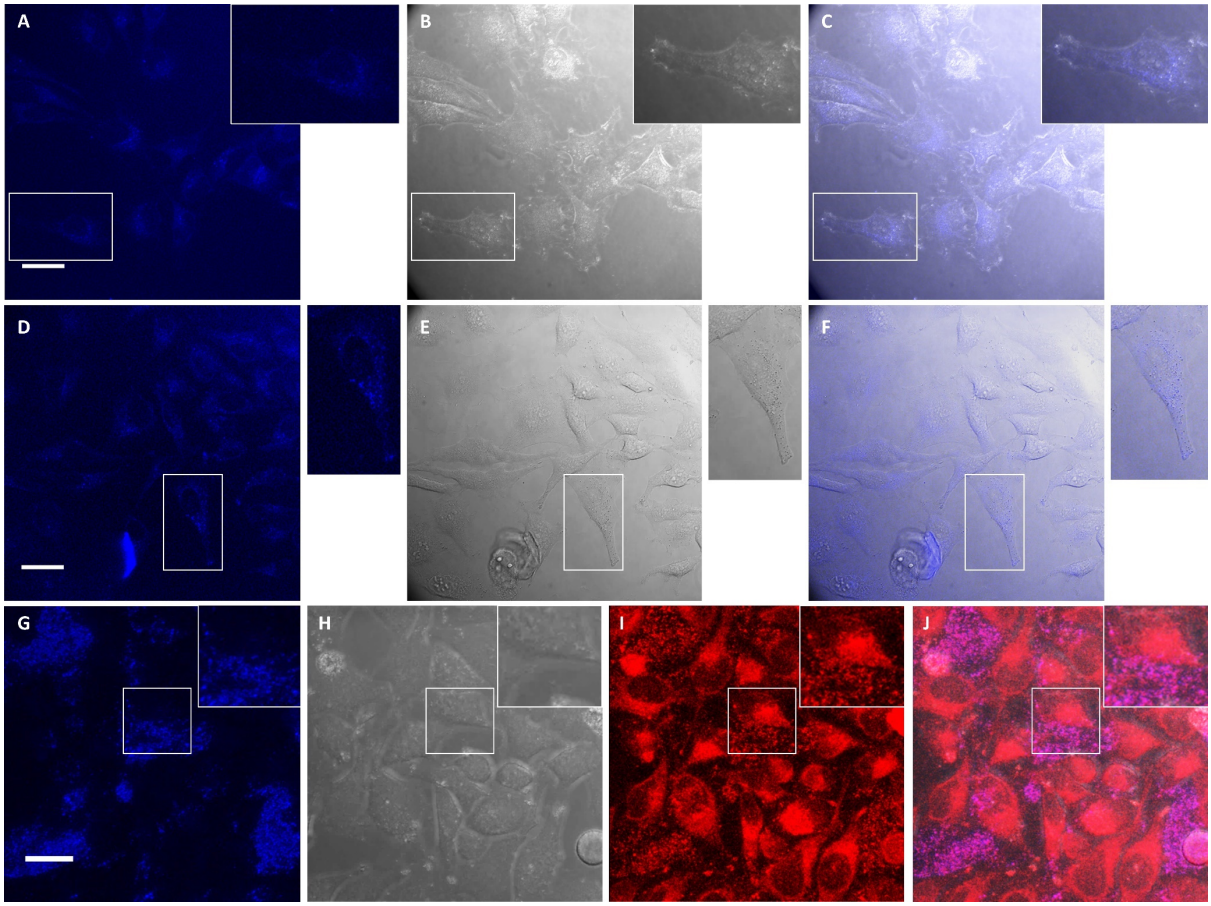

Figure S33. Evidence for the lack of observable PDHF fluorescence inside cells. (A-C) Live control HeLa cells; (A) blue channel. (B) brightfield transmitted light channel. (C) Overlay of images A-B. (D-F) Live HeLa cells incubated with FA-PEG-FA triblock nanofibers (100 µg/mL, L_n = 90 nm, L_w/L_n = 1.11, σ = 30 nm) for 45 minutes; (D) blue channel where PDHF fluorescence should be observed. (E) brightfield transmitted light channel. (F) Overlay of images D-E. (G-J) Live HeLa cells incubated with FA-BD-PEG-BD-FA pentablock nanofibers (50 µg/mL, L_n = 95 nm, L_w/L_n = 1.17, σ = 39 nm) for 1 h; (G) blue channel with observable extracellular PDHF fluorescence. (H) brightfield transmitted light channel. (I) BD fluorescence from FA-BD-PEG-BD-FA pentablock nanofibers. (J) Overlay of images G-I. Here you can see that extracellular BD fluorescence correlates with the expected PDHF fluorescence (purple), while intracellular BD fluorescence has no corresponding PDHF fluorescence (it remains red). PDHF fluorescence was measured at λ_{ex} = 405 nm, λ_{em} = 415-478 nm, while BD fluorescence was measured at λ_{ex} = 633 nm, λ_{em} = 640-700 nm. Scale bars are 20 µm.

References

1 M. Fernández, F. Javaid and V. Chudasama, *Chem. Sci.*, 2018, **9**, 790–810.

2 K. Siwowska, R. M. Schmid, S. Cohrs, R. Schibli and C. Müller, *Pharmaceuticals*, 2017, **10**, 72.

3 T. Yoshida, N. Oide, T. Sakamoto, S. Yotsumoto, Y. Negishi, S. Tsuchiya and Y. Aramaki, *J. Control. Release*, 2006, **111**, 325–332.

4 G. Liu, Y. Li, L. Yang, Y. Wei, X. Wang, Z. Wang and L. Tao, *RSC Adv.*, 2017, **7**, 18252–18259.

5 Q. T. Phan, M. H. Le, T. T. H. Le, T. H. H. Tran, P. N. Xuan and P. T. Ha, *Int. J. Pharm.*, 2016, **507**, 32–40.

6 D. Chávez-García, K. Juarez-Moreno, C. H. Campos, E. M. Tejeda, J. B. Alderete and G. A. Hirata, *J. Mater. Sci.*, 2018, **53**, 6665–6680.

7 F. de Jong, J. Pokorny, B. Manshian, B. Daelemans, J. Vandaele, J. B. Startek, S. Soenen, M. Van der Auweraer, W. Dehaen, S. Rocha and G. Silveira-Dorta, *Dye. Pigment.*, 2020, **176**, 108200.

8 S. Nayak, H. Lee, J. Chmielewski and L. A. Lyon, *J. Am. Chem. Soc.*, 2004, **126**, 10258–10259.

9 A. Reisch and A. S. Klymchenko, *Small*, 2016, **12**, 1968–1992.

10 M. Ajdary, M. A. Moosavi, M. Rahmati, M. Falahati, M. Mahboubi, A. Mandegary, S. Jangjoo, R. Mohammadinejad and R. S. Varma, *Nanomaterials*, 2018, **8**, 634.

11 X. H. Jin, M. B. Price, J. R. Finnegan, C. E. Boott, J. M. Richter, A. Rao, S. M. Menke, R. H. Friend, G. R. Whittell and I. Manners, *Science*, 2018, **360**, 897–900.

12 J. I. Lee, V. Y. Lee and R. D. Miller, *ETRI J.*, 2002, **24**, 409–414.

13 E. J. W. List, R. Guentner, P. Scanducci de Freitas and U. Scherf, *Adv. Mater.*, 2002, **14**, 374–378.

14 K. Li and B. Liu, *Polym. Chem.*, 2010, **1**, 252–259.

15 Y. Zhang, B. Liu and Y. Cao, *Chem.: Asian J.*, 2008, **3**, 739–745.

16 S. Roy, A. Gunukula, B. Ghosh and C. Chakraborty, *Sens. Actuators B Chem.*, 2019, **291**, 337–344.

17 C. Xue, S. Velayudham, S. Johnson, R. Saha, A. Smith, W. Brewer, P. Murthy, S. T. Bagley and H. Liu, *Chem. Eur. J.*, 2009, **15**, 2289–2295.

18 A. B. Pangborn, M. A. Giardello, R. H. Grubbs, R. K. Rosen and F. J. Timmers, *Organometallics*, 1996, **15**, 1518–1520.

19 P. Paul-Gilloteaux, X. Heiligenstein, M. Belle, M. C. Domart, B. Larijani, L. Collinson, G. Raposo and J. Salamero, *Nat. Methods*, 2017, **14**, 102–103.

20 F. De Chaumont, S. Dallongeville, N. Chenouard, N. Hervé, S. Pop, T. Provoost, V. Meas-Yedid, P. Pankajakshan, T. Lecomte, Y. Le Montagner, T. Lagache, A. Dufour and J. C. Olivo-Marin, *Nat. Methods*, 2012, **9**, 690–696.

21 J. J. Peterson, M. Werre, Y. C. Simon, E. B. Coughlin and K. R. Carter, *Macromolecules*, 2009, **42**, 8594–8598.

22 J. D. Lane, J. Lucocq, J. Pryde, F. A. Barr, P. G. Woodman, V. J. Allan and M. Lowe, *J. Cell Biol.*, 2002, **156**, 495–509.

23 Y. Olmos, L. Hodgson, J. Mantell, P. Verkade and J. G. Carlton, *Nature*, 2015, **522**, 236–239.